# An optimisation tool for minimising fuel consumption, costs and emissions from Diesel-PV-Battery hybrid microgrids

N. Rangel [a,*], H. Li [a,*], P. Aristidou [b]

[a] *School of Chemical and Process Engineering, University of Leeds, LS2 9JT, United Kingdom*
[b] *Dept. of Electrical Engineering, Computer Engineering and Informatics, Cyprus University of Technology, 3036, Cyprus*

## HIGHLIGHTS

- Improving the performance of diesel generators gives economic and environmental benefits for hybrid microgrids planning.
- Better interaction among diesel generators and renewable energy for rural electrification can be achieved using cost optimisation tools.
- Including biofuel blends in a cost optimisation tool allows for assessing locally produced fuels for diesel substitution.
- $PM_{2.5}$ and $NO_X$ emissions influence the biofuel selection to be used within hybrid microgrids.
- Cost-benefit analysis helps to determine the best microgrid system configuration, considering financial and environmental aspects.

## ARTICLE INFO

## ABSTRACT

Diesel generators (diesel gensets) are widely used within microgrid (MG) and off-grid systems for rural electrification, particularly in developing countries. The sizing and selection techniques during the MG planning stage are a key for maximising cost-effectiveness and minimising environmental impacts. This becomes more important for hybrid mini-grid systems when photovoltaic (PV) electricity generation and other renewable energies are included in the system as special attention is needed to limit the genset's output power, to keep it within the recommended operating range. This paper presents a cost optimisation model, centred on the generators performance, within diesel/PV/battery MGs, for minimising the MG's operating costs and environmental impact. The model considers fuel consumption equations adapted for castor oil-diesel (COD) blends and two major pollutant emissions (NOx and $PM_{2.5}$), which are not considered in other optimisation models. The optimisation was implemented for high, medium, and low electricity demand scenarios, with eight possible system configurations, for the Lindi Region of Tanzania as it belongs to one of the five countries with the lowest electricity access in sub-Saharan Africa (SSA). An economic assessment was done to compare the Levelized Cost of Energy (LCOE) of the system configurations. The impact of the fuel price and pollutant emission costs on the fuel selection was investigated using sensitivity analysis. The results confirmed that for specific electricity demand each scenario requires a unique set of diesel generators and the selection is affected by the PV share and the battery energy storage (BES) units included. The best LCOE for the high, medium, and low electricity demand scenarios were 0.43£/kWh, 0.42£/kWh, and 0.45£/kWh, respectively. The sensitivity analysis revealed that the pollutant emission costs have a significant impact on LCOE for the different fuel choices whereas the variation of fuel prices has a minimal effect unless the diesel price increased by 100%.

## 1. Introduction

Expanding electricity access in rural areas of developing countries for achieving the Sustainable Development Goal 7 (SDG7[1]) [1] represents a challenging task, as 840 million people around the world have no access to electricity. The majority of them, around 600 million people, live in sub-Saharan Africa and half of that population is distributed across Nigeria, DR Congo, Ethiopia, Tanzania, and Uganda.

To overcome this situation, the Rural Electrification Agency (REA) is implementing a large-scale electrification strategy, that considers MG deployment and standalone systems, as the least-costly option for providing the power required by 2030 [2]. According to the report presented by the Energy Sector Management Assistance Program (ESMAP) [3], there are about 19,163 MGs globally and most of them are diesel-fuelled. Of those, nearly 1,500 are located in sub-Saharan Africa. In the coming years, the implementation of more than 7500 MGs will bring a significant shift from diesel-based to solar and solar-hybrid systems. It has been estimated that MG deployment will have a sharp growth in Africa and more than 4,000 will be installed over the next couple of years [4]. In developing countries, MGs consist mostly of small diesel- and hydro-powered systems serving 200 to 2000 people. Though diesel generators are commonly used in MGs to electrify off-grid areas [5–8], a major problem remains within the planning stage of hybrid MGs, which is to accurately predict the performance of diesel generators, particularly during low load demand periods. Even though diesel generators are an important element that brings stability and reliability to the systems, they are commonly seen and modelled as "a black box" that leads to high operating costs and environmental impact due to their excessive fuel consumption. This paper presents a cost-optimisation model developed for a diesel/PV/BES hybrid MG considering the effect of castor oil-diesel blends to reduce fossil fuel consumption while minimising the economic and environmental impact of the system.

Although diesel generators are widely used in off-grid electric systems their poor performance is a common issue that occurs when the gensets operate at low load conditions, affecting the overall system's operation. As mentioned by Sinn [9], using a high-power diesel engine, able to meet the required power during peak demand, gives high operation and maintenance costs when operating the genset at a low load. The low load working mentioned was caused by inappropriate genset sizing and selection. Generally, the decision on genset sizing and selection is made to meet the total or peak load demand considering the energy loss during transmission and distribution (line losses) [10], to guarantee reliable electricity supply at peak demand. According to Diaz et al. [11], the required power (size) of a diesel generator is calculated to cover a peak demand plus a security margin of 10 %. This technique gives over-sized generators that rarely operate near their nominal power (their optimal performance), especially during low-demand periods. Literature shows that some systems operate below 25 % [11] or between 30 % and 60 % of the maximum load [12]. Other systems operate between 6 % and 33 % of the gensets rated load capacity and their specific fuel consumption might be up to five times greater than the manufacturer's specifications [13]. Soto [13] concluded that generator sizes with better load matching could reduce fuel consumption while improving reliability and lowering maintenance needs. Similarly, the studies done by Schnitzer [14] in 36 municipalities in Haiti revealed that the size of the generators, relative to the load demand, is a significant factor causing a high fuel cost. The author pointed out that it would be beneficial to replace those oversized generators with smaller-scale units. Replacing oversized generators could also benefit hybrid systems design as the interaction of diesel generators with renewable energy technologies could affect the operation of the system. For example, the PV/diesel system in the province of Jujuy, Argentina, presented by Diaz et al. [15] illustrates that when PV arrays are undersized the diesel generators ought to meet the demand, increasing the operating cost due to the increased fuel consumption. Also, the results presented by Yamegueu et al. [8] showed that a high share of PV in a low load system does decrease the optimal functioning of a genset (below 62 % of its rated power); therefore, they recommend a design that allows the genset to operate near its nominal power. A similar situation is found in African countries where a poor demand prediction results in having oversized MGs that lead to a low load operation and thus poor performance. To overcome that situation, Booth et al. [16] suggest that an ideal solution should consider the appropriate sizing of the systems during the design phase. For a hybrid system sizing should consider the renewable-diesel

balance that allows for maximising the use of renewable by the selection of energy sources to supply loads separately or to meet a high demand by combining all the sources at the same time [17]. The goal is to avoid a low load operation of the diesel generator and hence improve the overall system performance.

The optimum design (sizing) of MGs have been conducted and reported by [7,8,11,18]. A review made by Mellit et al. [19] presents the application of artificial intelligence techniques such as Neural Networks and Genetic Algorithms among others for sizing PV systems. Their work includes a section with studies for sizing hybrid PV systems for optimum selection of solar array panels, wind turbines, and battery configurations. It also includes more than one study for finding the optimal total capital cost depending on the loss of power supply probability. According to Bernal-Agustin et al. [20], the optimum design is usually carried out by minimizing the Net Present Cost (NPC) or the Levelized Cost of Energy (LCOE) of a project using simulation and optimisation software tools available for hybrid systems. Their study mentions that the most-used optimisation software is the Hybrid Optimization Model for Electric Renewables (HOMER) developed by the National Renewable Energy Laboratory (NREL). The review made by Connolly et al. [21] of 37 computer tools, commonly used to analyse the integration of renewable energy in different systems, revealed that no energy tool addresses all aspects of the integration. However, in their review, HOMER appeared as one of the most used tools for stand-alone applications. Similarly, in the review made by Sinha [22], where 19 optimisation software tools were analysed, it was indicated that HOMER has been used extensively for hybrid renewable energy system optimisation, regardless of the limitations noted by the authors. In Suman's et al. recent work [23] for hybrid system optimisation in rural areas, HOMER was shown as one of the software tools efficiently used for sizing hybrid renewable energy systems, but the authors appeal to a modern technique in optimal sizing of renewable energy sources that implements evolutionary algorithms such as Particle Swarm Optimisation (PSO), Differential Evolution, Genetic Algorithm (GA), Simulated Annealing (SA), and others. Their work presented a swarm-based optimisation method for allowing the users to employ customised constraints and avoid the existing limitations from available optimisation tools.

Despite the awareness of the importance of re-sizing diesel generators only a few authors have studied the benefits of using more than one diesel generator for optimum matching in genset size, power output and load demand. Alramlawi et al. [24] observed that installing three diesel generators instead of only one, in combination with a PV array without a battery was more efficient in the MG system of their study. In the study by Pelland et al. [25], fuel savings were reported by adding PV arrays, reducing dump loads and using smaller diesel generators. The authors suggested that further optimisation for genset sizing and system would contribute to more fuel savings that would be translated into less greenhouse gas (GHG) emissions. Another study that explored the benefits of operating two smaller engines for diesel-based standalone applications was presented by Kusakana [26]. The author reported fuel savings of around 30 % if two diesel generators are used in parallel instead of a single unit, as one of them operates at a high load factor and the second one has reduced operating time. Also, with the optimisation techniques used by Jesper Knudsen et al. [27], gradient search approach and genetic algorithm approach, potential fuel savings from 0.1 to 3 % could be achieved in a multiple diesel generator independent power producer power plant.

Literature shows that even when using novel optimisation algorithms such as the Particle Swarm Optimisation-Grey Wolf Optimiser used by Suman et al.[23], the performance of diesel generators receives little attention and their fuel consumption estimation still relies on the linear equation presented in 1986 by Reiniger [28]:

$$q(t) = a \cdot P(t) + b \cdot P_r \tag{1}$$

Where, $q(t)$ is hourly fuel consumption in l/kW; $P(t)$ is the power generated by the generator in kW; $P_r$ is the rated/nominal power of the

generator in kW; a and b are the model coefficients in l/kWh.

The equation (1) has been used ever since by different authors [8,29–31] as part of the "black box" modelling technique for including diesel generators in MG design. A similar equation appeared in the Techno-economic analysis presented by Rohani [32], which is the one implemented by HOMER. The equation allows for adjusting the "a" and "b" coefficients presented by Reiniger as "a" can be estimated if at least two fuel consumption parameters at different loads are known, and "b" can be computed from the no-load consumption divided by the rated power of the generator [33,34]. Some authors prefer quadratic equations instead, as according to Ashock [35] the fuel consumption of a diesel generator is well represented by a second-order polynomial if it operates near its rated power. Agarwal et al. [36] used a quadratic expression in which coefficients were determined from manufacturer's specifications, the same way as reported by [35]. Pelland et al. [25] also selected a quadratic equation but they emphasized that the fuel analysis is very sensitive to the type of fit applied, especially for loads below 25 % rated power, producing large uncertainties in the final fuel estimation. The work presented by Gan et al. [37] estimated the fuel consumption through a third-order polynomial function, using empirical data instead of manufacturer's data, but they revealed that more work should be done to have a better generator sizing.

The review above shows that though there are various techniques for sizing, optimisation, and estimating the fuel consumption of diesel generators operating in hybrid systems, none of the studies has considered the scenario of using vegetable oil-diesel blends to study the performance of diesel generators in MGs. There are a number of hybrid Microgrid studies involving biomass or biofuels but those are based on using solid biomass gasification technologies which are fed into a gas engine or a diesel engine [38–41]. The use of vegetable oil-diesel blends in a diesel generator is new. Therefore, developing a cost optimisation model from the engine's perspective, that allows for better sizing and prediction of the performance of diesel generators in MGs to compare the use of vegetable oils (and other liquid fuels) and diesel in terms of operating cost and environmental impact is needed. This paper aims to propose a cost optimisation model incorporating fuel consumption of diesel generators with castor oil-diesel blend scenario and environmental costs. Finally, the paper also explains why the model aims to limit the operating range of diesel generators to avoid their low load operation and improve their performance, as they do influence the optimal configuration of stand-alone systems as concluded by Bilal et al. [42].

From the information provided above, this paper's contribution can be listed as follows:

- Highlight the importance of considering diesel generators as a key element in cost optimisation models, to improve their performance for reducing their fuel consumption and operating costs in MG.
- Present new fuel estimation equations that enable the assessment of locally produced biofuels, for diesel substitution in MG for rural electrification.
- Demonstrate that using diesel generators within the recommended limit benefits their sizing and interaction with renewable energy sources, which in turn benefits MG planning.

This paper has been divided into 7 sections. Section 1 presents an introduction to the identified gap and proposed solution for improving MG planning stage and the performance of diesel generators through a cost optimisation problem, to reduce operating costs and pollutant emissions for rural electrification in SSA countries. Section 2 presents the proposed cost optimisation model, starting with an overview of the model's characteristics, followed by the model's objective function and constraints discussed in section 2.1 and section 2.2. Section 2.3 and 2.4 present the inputs used to test the model and the relevant equations of the economic assessment of the optimised findings. Section 3 describes the scenarios created for testing the applicability of the cost model. The electricity demand profiles are included in section 3.1, whereas section 3.2 and 3.3 are dedicated to the PV scenarios. Section 4 gives an exemplar application of the cost optimisation model given specific PV installed capacity, PV performance, and battery capacity for three electricity demand profiles. In Section 5 an economic assessment as well as a cost-benefit analysis of the optimised MG configurations found in Section 4 are included. After that, a sensitivity analysis for the MG selected through the cost-benefit analysis is included in Section 6. Finally, Section 7 presents the conclusions of this work.

## 2. Configuration of the cost optimisation model

In this section, we will present a cost optimisation model developed to assess the selection of diesel generators for eight microgrid system configurations. The selection depends on the performance of each generator, the pollutant emission generated and the fuel options. For the assessment, the model considers three Tanzanian electricity demand profiles. The proposed Linear Mixed Integer Problem (LMIP) cost optimisation model was implemented in Python with the Gurobi optimisation solver [43]. The model minimises the yearly cash flow expenses of a diesel/PV/BES hybrid MG by selecting the optimum size and number of diesel generators, and the optimum biofuel blend to reduce fuel consumption and pollutant emissions. A description of the indices, sets, parameters, and variables of the model is included in the supplementary material for enhanced readability of the paper.

### 2.1. Objective function

The objective function of the proposed model is to minimize the total cost of investment, operation, maintenance, and replacement, for a specific standalone hybrid MG. The analysis is performed over the entire duration of the MG lifetime and is split over years, months, and hours of analysis. The mathematical representation is:

$$\min C^{cap} + C^{op} + C^r + C^{mnt} \tag{2}$$

where $C^{cap}$ is the capital cost, $C^{op}$ the operating cost, $C^r$ the replacement cost, and $C^{mnt}$ the maintenance cost. Each term is explained below after presenting the sets and indexes included in the model:

$P$ is the set of project analysis periods in years (25 Years),

$M$ is the set of months within the analysis period (12 Months),

$T$ is the set of operating periods (24 h),

$G$ is the set of candidate diesel generators considered in the model (7 generators of different sizes),

$B$ is the set of candidate fuel blends (4 blends).

The elements belonging to the sets above are represented with the following indexes: $p$ for year, $m$ for month, $t$ for operating period, $g$ for genset, and $bld$ for fuel blend. These annotations apply to the whole paper.

$C^{cap}$a): this term corresponds to the initial investment, given by

$$C^{cap} = \sum_{g \in G} C_g^{gen} + C^{PV} + C^{inver} + C^{batt} \tag{3a}$$

$$C_g^{gen} = g_g^{upc} \cdot P_g^{gen_{max}} \cdot \max\left(s_{g,t}\right) \forall g \tag{3b}$$

$$C^{PV} = \text{cost}^{PV} \cdot inst^{PV} \tag{3c}$$

$$C^{inver} = \text{cost}^{inver} \cdot inst^{PV} \tag{3d}$$

$$C^{batt} = \text{cost}^{batt} \cdot Cap^{batt} \tag{3e}$$

where $C_g^{gen}$, $C^{PV}$, $C^{inver}$, and $C^{batt}$ are the initial investment costs of the selected diesel generators, PV system, inverter, and battery system, respectively. The upfront cost per genset in £/kW is represented by $g_g^{upc}$, and $P_g^{gen_{max}}$ is the genset's maximum power indicated for continuous operation in kW. The binary decision variable $s_{g,t} \in \{0, 1\}$ indicates if a diesel generator is selected or not. The costs of the PV and the inverter in
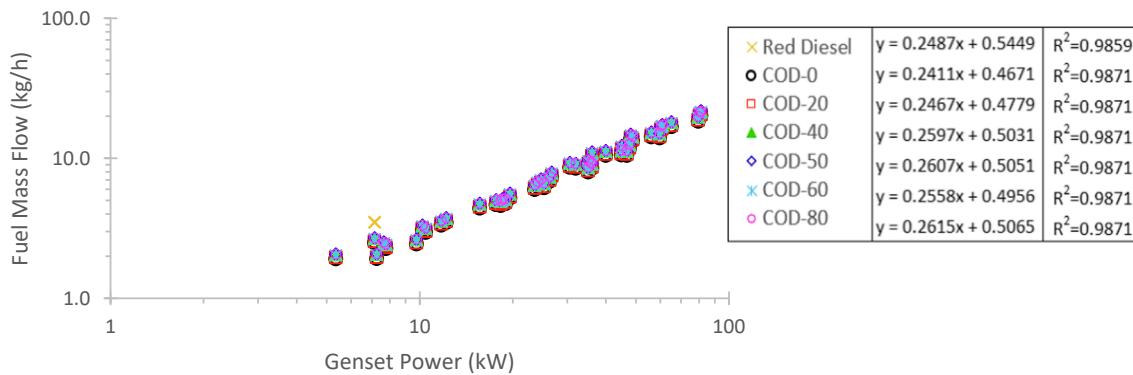
**Fig. 1.** Mass-based fuel consumption against generated power for selected diesel generators.

**Table 1**
Diesel and Castor oil-diesel blends density values at different temperatures.

| Fuel | Density [kg/l] | Fuel Temperature [°C] |
|---|---|---|
| Red Diesel[3] | 0.86 | 15 |
| COD-0 | 0.830 | 30 |
| COD-20 | 0.849 | 30 |
| COD-40 | 0.894 | 30 |
| COD-50 | 0.897 | 30 |
| COD-60 | 0.880 | 60 |
| COD-80 | 0.900 | 70 |

3 From manufacturer's specifications. The density of the red diesel (0.86 kg/l) is higher than the density value reported for COD-0 (0.83 kg/l) due to the different fuel temperatures at which their densities were tested.

£/kW are represented by cost$^{PV}$ and cost$^{inver}$. The battery cost is indicated in £/kWh by cost$^{batt}$. The installed PV in kW is *inst$^{PV}$*, similarly *Cap$^{batt}$* is the installed battery system capacity in kWh calculated using the power storage capacity sizing equation (4)[2] adapted from the Handbook on Battery Energy Storage System [44], given by

$$BESSCapacity[kWh] = \frac{\text{Power required [kW]·duration required [h]}}{\text{depth of discharge [%]·battery efficiency [%]}} \quad (4)$$

*C$^{op}$*b): this term corresponds to the total operational costs derived from the fuel consumption and emissions of the diesel generators for one year of operation (*pdays* $\sim$ 365$^{\circ}$), given by

$$bp_{bld} = \text{dieselprice·}\left(\frac{bld}{100}\right) + \text{castoroilprice·}\left(1 - \frac{bld}{100}\right) \quad (5c)$$

$$bld \in \{100, 80, 60, 50\}$$

where $bp_{bld}$ is the blend purchase price in £/litre calculated.

$$Fu_{bld,g,t} = \left(\frac{a_{bld}·P_{g,t}^{gen} + b_{bld}}{\rho_{bld}}\right)·k_{g,t,bld} \forall bld, g, t \quad (5d)$$

The total fuel consumption per genset in l/h is $Fu_{bld,g,t}$, where $a_{bld}$ and $b_{bld}$ are the coefficients found for each fuel blend, and $\rho_{bld}$ is the density of each blend in kg/l. The decision variables $P_{g,t}^{gen}$ and $k_{g,t,bld} \in \{0,1\}$ determine the genset output power and the fuel selection in every operating period, respectively. In (5d) the coefficients $a_{bld}$ and $b_{bld}$ correspond to the slope and the Y-intercept of the linear regression that appears in Fig. 1, respectively.

Fig. 1 shows the correlation between mass fuel consumption and genset power output for seven different fuels/blends. The original diesel fuel consumption data were collected from the specifications of 83 diesel generators from 5 different suppliers/manufacturers within a 6 kVA to 100 kVA range. Some manufacturers present the fuel consumption in g/kWh but the volumetric representation in l/h is commonly used. The reported values vary from full prime rating to 25 % genset's prime rating. Most manufacturers only report the fuel flow at prime and 75 % or 70 % prime rating. Therefore, only the genset models having more than one fuel consumption specification in l/h were selected. The se-

$$C^{op} = pdays\left(\sum_{t \in T}\sum_{g \in G}\sum_{bld \in B} C_{bld,g,t}^{fuel} + \sum_{t \in T}\sum_{g \in G}\sum_{bld \in B} C_{bld,g,t}^{CO_2e} + \sum_{t \in T}\sum_{g \in G}\sum_{bld \in B} C_{bld,g,t}^{NOx} + \sum_{t \in T}\sum_{g \in G}\sum_{bld \in B} C_{bld,g,t}^{PM_{2.5}}\right) \quad (5a)$$

where, for each operating hour, generator, and blend, $C_{bld,g,t}^{fuel}$ fuel cost, $C_{bld,g,t}^{CO_2e}$ carbon dioxide equivalent (CO$_2$e) emission cost, and $C_{bld,g,t}^{NOx}$ and $C_{bld,g,t}^{PM_{2.5}}$ are the emission costs for nitrogen oxides (NO$_x$) and particulate matter (PM$_{2.5}$), respectively. Equations (5b), fuel costs, are comprised of the fuel purchase price $bp_{bld}$ and fuel consumption $u_{bld,g,t}$, which are calculated using equations (5c) and (5d) respectively.

$$C_{bld,g,t}^{fuel} = bp_{bld}·Fu_{bld,g,t} \forall bld, g, t \quad (5b)$$

lection includes engines of different sizes from Perkins, Deutz, Iveco, and Yanmar. The volumetric fuel consumption data obtained was converted into its mass-based form (kg/h) using the typical density value for red diesel at 15 °C [45]. The red diesel density at 15 °C was chosen as manufacturers report the fuel consumption complying with the red fuel specification standard BS2869 [46]. For castor oil-diesel blends, the density of each castor oil-diesel blend (COD) at the testing temperatures, as shown in Table 1, was used to convert the original diesel data to the corresponding fuel blend. The COD-0 is the pure red diesel but tested at 30 °C so there are two red diesel densities (15 and 30 °C). Then linear regressions were conducted to find the fuel consumption equations for each fuel type. Fig. 1 shows the mass-based fuel consumption data with linear regression equations and R$^2$ for diesel and castor oil-diesel blends, the mass-based fuel values are summarised in Table S6 included in the supplementary material. There is a gap in fuel consumption data

---

2 The equation is used for sizing the power storage capacity when renewable integration, peak shaving or MGs applications are considered.
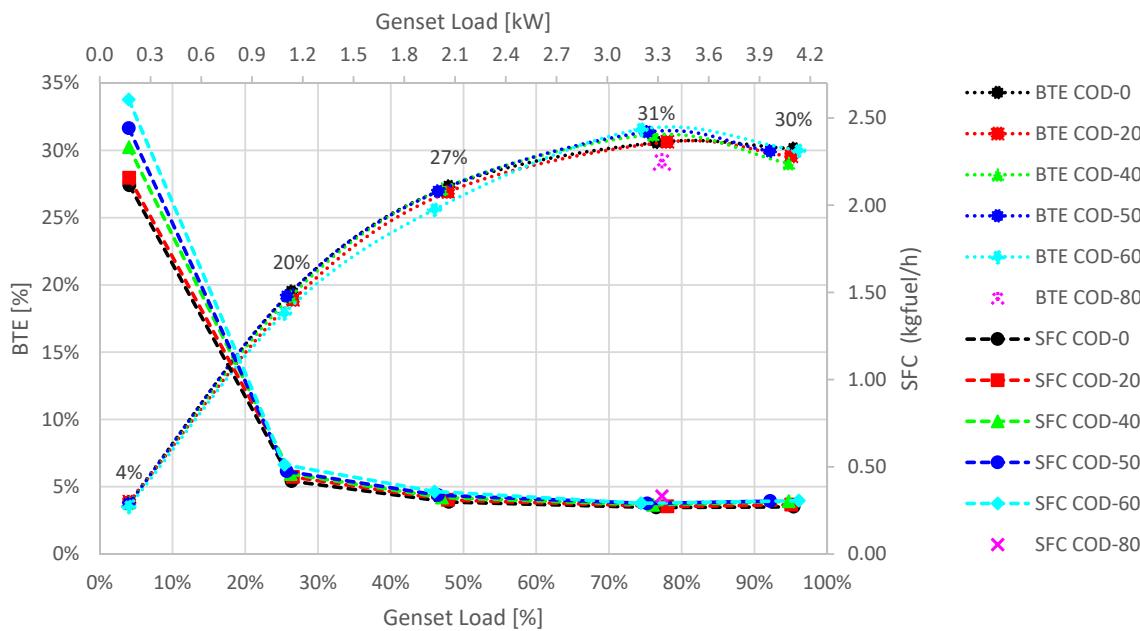
**Fig. 2.** BTE and SFC curves from a diesel generator running with castor oil-diesel (COD) blends.

between 65 and 80 kW but the over trends showed a good linear behaviour for all the fuels.

$$C_{bld,g,t}^{CO_2e} = \text{tax}^{\text{carbon}} \cdot bEF_{bld} \cdot Fu_{bld,g,t} \forall bld, g, t \tag{5e}$$

$$bEF_{bld} = EF^{diesel} \cdot \left(\frac{bld}{100}\right) + EF^{biofuel} \cdot \left(1 - \frac{bld}{100}\right)$$

$$bld \in \{100, 80, 60, 50\} \tag{5f}$$

where $tax^{carbon}$ is the cost in £/kgCO₂e for CO₂e emissions and $bEF_{bld}$ is the fuel blend emission factor in kgCO₂e/litre for specific fuel blends as calculated with (4f). $EF^{diesel}$ and $EF^{biofuel}$ are the diesel and biofuel corresponding emission factors, also in kgCO₂e/litre.

$$C_{bld,g,t}^{NOx} = ecost^{NOx} \cdot e_{bld,g,t}^{NOx} \forall bld, g, t \tag{5 g}$$

$$e_{bld,g,t}^{NOx} = size_g^{eng} \cdot glfa_g \cdot BEF_g^{NOx} \cdot EFA_{bld}^{NOx} \cdot k_{g,t,bld} \forall bld, g, t \tag{5 h}$$

where $ecost^{NOx}$ is the NOx emissions cost in £/gNO$_X$. $e_{bld,g,t}^{NOx}$ represents the NOx emissions per hour per genset, $size_g^{eng}$ is the genset's engine prime power in kW, while $glfa_g$ and $BEF_g^{NOx}$ are the load factor adjustment and the NO$_x$ baseline emission factor in g/kWh, respectively, according to the methodology for estimating pollutant emissions for non-road machinery [47]. The NO$_x$ emission factor adjustment $EFA_{bld}^{NOx}$ is the coefficient found from experimental work for each biofuel blend.

$$C_{bld,g,t}^{PM_{2.5}} = ecost^{PM_{2.5}} \cdot e_{bld,g,t}^{PM_{2.5}} \forall bld, g, t \tag{5i}$$

$$e_{bld,g,t}^{PM_{2.5}} = size_g^{eng} \cdot glfa_g \cdot BEF_g^{PM_{2.5}} \cdot EFA_{bld}^{PM_{2.5}} \cdot k_{g,t,bld} \forall bld, g, t \tag{5j}$$

where $ecost^{PM_{2.5}}$ is the PM₂.₅ emissions cost in £/gPM₂.₅. $e_{bld,g,t}^{PM_{2.5}}$ represents the PM₂.₅ emissions per hour per genset, $BEF_g^{PM_{2.5}}$ is the PM₂.₅ baseline emission taken from [47], and $EFA_{bld}^{PM_{2.5}}$ is the emission factor adjustment coefficient calculated from experimental work for each biofuel blend.

$C^r$c): this term refers to the cost of replacing the diesel generators and is given by

$$C^r = \sum_{g \in G} (0.88C_g^{gen}/2) \cdot \sum_{m \in M} replace_{g,m}^{engine} + \sum_{g \in G} (0.88C_g^{gen}/2) \cdot \sum_{m \in M} replace_{g,m}^{alternator} \tag{6a}$$

$$replace_{g,m}^{engine} = \left\{ \frac{1 if Hgcm_{g,m} \geq glf_g \forall g, m}{0 otherwise} \right\} \tag{6b}$$

$$replace_{g,m}^{alternator} = \left\{ \frac{1 if Hgcm_{g,m} \geq 20000 \forall g, m}{0 otherwise} \right\} \tag{6c}$$

where $replace_{g,m}^{engine}$ and $replace_{g,m}^{alternator}$ indicate the decision of replacing the engine or the alternator of genset $g$ in month $m$, respectively, and $glf_g$ represents the lifetime of each engine.

$C^{mnt}$d): this term represents the maintenance required for the gensets selected,

$$C^{mnt} = bp_{bld=100} \left( \sum_{g \in G} mntdays_g \left( \frac{(a_{bld=100}P_g^{gen_{max}} + b_{bld=100}) \cdot max(s_{g,t})}{\rho_{bld=100}} \right) \cdot K_{p=1,bld} \right) + servc \left( \sum_{g \in G} P_g^{gen_{max}} \cdot max(s_{g,t}) \cdot K_{p=1,bld} \right) \tag{7a}$$

$$mntdays_g = \left\{ \frac{12 \cdot (t/4) if k_{p=1,bld=100} \forall g}{365 \cdot (t/4) otherwise} \right\} \tag{7b}$$

where $bp_{bld=100}$ is the diesel price in £/l, $mntdays_g$ represents the estimated maintenance days, depending on the type of fuel used during the operating periods. $P_g^{gen_{max}}$ is the prime power of the selected gensets in kW, as indicated by $s_{g,t}$, and $K_{p=1,bld}$ represents the blend selected during the analysis period. The annual service cost is represented by $servc$ in £/kW, based on the operation and maintenance cost from the MG REopt LCOE Results Explorer [48].

### 2.2. Model constraints

The constraints below were needed to account for the operational limitations of the energy sources (i.e., diesel generators, PV, and BES).

The system power balance to meet the load demand at each hour of the day $d_t$, considering the PV system output power $P_t^{RE}$ and the power

**Table 2**

Input parameters for the optimisation model.

| Model Input | | Source |
|---|---|---|
| Diesel price (£/litre) * | 0.88 | Tanzania Diesel prices [52]. |
| Castor oil price (£/litre) * | 0.44 | Tanzania Castor Oil Prices [53]. |
| Carbon tax (£/kgCO₂e) * | 0.0075 | Carbon Pricing Dashboard [54]. |
| Diesel: average biofuel blend conversion factor (kg CO₂e/litre) | 2.51233 | UK Government Conversion Factors for greenhouse gas reporting [55] |
| Biofuel conversion factor (kg CO₂e/litre) | 0.02529 | Experimental data from Castor oil-diesel blends engine tests. |
| PM₂.₅ emission cost (£/g) * | 0.0527 | The true cost of fossil fuels: Externality cost assessment methodology [56]. |
| NOx emission cost (£/g) * | 0.0089 | |
| Genset upfront cost (£/kW) * | 614.72 (genset size < 100 kW) 388.00 (genset size greater than 100 kW) | Detailed Cost Models and Benchmarks [57]. |
| Genset maintenance cost (£/kW) * | 19.02 | MG Load and LCOE Modelling Results [48]. |
| PV cost (£/kWp) * | 1,673.74 | Tariff Considerations for Micro-Grids in Sub-Saharan Africa [58]. |
| Inverter cost (£/kW) * | 912.95 | |
| Lead-acid battery cost (£/kWh) * | 60.86 | State of the global MG Market Report 2020 [59]. |
| Li-ion battery cost (£/kWh) * | 133.90 | |
| Repurposed battery cost (£/kWh) | 66.95 | Calculated from Li-ion price. |

* Prices converted to £ from their original values in USD, considering the average exchange rate history of 1 USD=0.76079 GBP (Dec-May 2022) [60].

supplied ($P_t^{batt_{dischar}}$) or consumed ($P_t^{batt_{char}}$) by the batteries, both in kW is given by

$$\sum_{g \in G} P_{g,t}^{gen} + P_t^{RE} + P_t^{batt_{dischar}} - P_t^{batt_{char}} = d_t \forall t \quad (8a)$$

A load demand security margin $D_t$ is considered, where the maximum power from the selected gensets $P_g^{gen_{max}}$ and the maximum battery discharging power $P_t^{battmax_{dischar}}$ can be used according to (8b).

$$\sum_{g \in G} \left( P_g^{gen_{max}} \cdot w_{g,t} \right) + P_t^{RE} + P_t^{battmax_{dischar}} \geq D_t \forall g, t \quad (8b)$$

The constraints related to the selection of the diesel generators are given by

$$\sum_{g \in G} s_{g,t} \leq U \quad (9a)$$

$$P_{g,t}^{gen} \geq P_g^{gen_{min}} \cdot w_{g,t} - genslack_{g,t} \forall g, t \quad (9b)$$

$$P_{g,t}^{gen} \leq P_g^{gen_{max}} \cdot w_{g,t} \forall g, t \quad (9c)$$

$$s_{g,t} \geq w_{g,t} - w_{g,t-1} \forall t > 0, g \quad (9d)$$

$$s_{g,t} - w_{g,t} \geq 0 \forall t, g \quad (9e)$$

where the binary decision variable $s_{g,t} \in \{0, 1\}$ determines which genset is selected without exceeding the maximum number represented by $U$. $P_g^{gen_{min}}$ refers to the lowest acceptable genset output power in kW. This limit was investigated because sometimes in optimisation the limit is set to 30 % of the genset's prime power [24]. However, according to [49] the optimum genset operating range goes from 70 to 89 % of its rated power and [50] mentions that the highest efficiency of the diesel engine occurs above 60 % load. The model considers the operating limits

determined by the specific fuel consumption (SFC) and the brake thermal efficiency (BTE) results from experimental work using a 6kVA diesel generator. The optimal operating limits are represented by the region where the lowest SFC values and the highest BTE occur, above 60 % of the genset's prime power, as shown in Fig. 2. The equations for the calculation of BTE and SFC are in the supplementary materials III (equations (18) and (19)). A key message from Fig. 2 is that the genset load factor needs to be at 60 % and above to achieve maximum BTE and minimum SFC. This threshold is not affected by different fuel blends.

The constraints related to the selection of the fuel blend are given by

$$\sum_{bld \in B} k_{g,t,bld} \leq 1 \forall g, t \quad (10a)$$

$$w_{g,t} = \max \left( k_{g,t,bld} \right) \forall g, t \quad (10b)$$

where (10a) and (10b) ensure that the gensets only operate with one type of fuel blend.

The constraints related to the battery are given by

$$E_t^{batt} = E_{t-1}^{batt} + \left( \eta^{batt} \cdot P_t^{batt_{char}} - \frac{P_t^{batt_{dischar}}}{\eta^{batt}} \right) \forall t \quad (11a)$$

$$E_t^{batt} \leq SoC^{max} \cdot Cap^{batt} \forall t \quad (11b)$$

$$E_t^{batt} \geq SoC^{min} \cdot Cap^{batt} \forall t \quad (11c)$$

$$E_0^{batt} = SoC^{max} \cdot 0.8 Cap^{bat} \quad (11d)$$

$$E_{23}^{batt} = E_0^{batt} \quad (11e)$$

$$P_t^{batt_{char}} \geq 0 \cdot char_t \forall t \quad (11f)$$

$$P_t^{batt_{char}} \leq P^{batt_{max}} \cdot char_t \forall t \quad (11g)$$

$$P_t^{batt_{dischar}} \geq 0 \cdot dischar_t \forall t \quad (11h)$$

$$P_t^{batt_{dischar}} \leq P^{batt_{max}} \cdot dischar_t \forall t \quad (11i)$$

$$P^{batt_{max}} = Cap^{batt} / 5 \quad (11j)$$

$$char_t + dischar_t \leq 1 \forall t \quad (11k)$$

where $E_t^{batt}$ is the energy available from the batteries at a specific operating period. The battery efficiency is represented by $\eta^{batt}$, $SoC^{max}$ and $SoC^{min}$ are the battery's maximum and minimum state of charge. The charging and discharging battery periods are determined by the binary decision variables $char_t \in \{0, 1\}$, and $dischar_t \in \{0, 1\}$.

Finally, the constraints on the replacement of the diesel generators are given by

$$Hgcm_{g,m} \geq Hgm_g \cdot \left( 1 - replace_{g,m}^{engine} \right) \forall g, m \quad (12a)$$

$$Hgcm_{g,m} \leq glf_g \cdot \left( 1 - replace_{g,m}^{engine} \right) \forall g, m \quad (12b)$$

$$Hgcm_{g,m} \geq Hgm_g \cdot \left( 1 - replace_{g,m}^{alternator} \right) \forall g, m \quad (12c)$$

$$Hgcm_{g,m} \leq 20000 \cdot \left( 1 - replace_{g,m}^{alternator} \right) \forall g, m \quad (12d)$$

$$Hgd_g = \sum_{t \in T}^1 w_{g,t} \forall g \quad (12e)$$

$$Hgm_g = 30 \cdot Hgd_g \forall g \quad (12f)$$

$$Hgcm_{g,m} = m \cdot Hgm_g \forall g, m \quad (12\,g)$$

$$Hga_g = Hgcm_{g,m} \forall g, m = 12 \quad (12\,h)$$
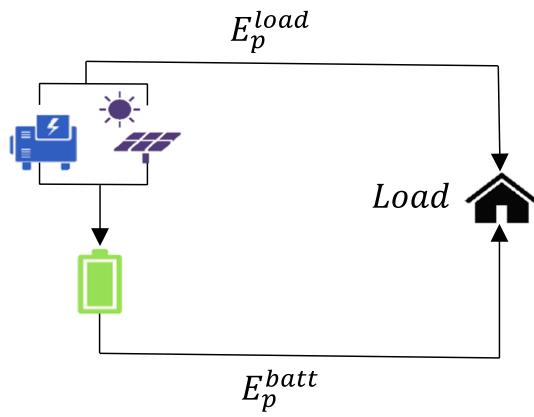
**Fig. 3.** Electricity flow diagram for a genset/PV/battery hybrid system.

where $Hgcm_{g,m}$, $Hgm_g$, $Hgd_g$, and $Hga_g$ are the monthly cumulative, monthly, daily, and annual operating hours of the gensets, respectively. The binary decision variable $w_{g,t}$ indicates if a genset is operating or not during the daily or monthly operating periods.

### 2.3. Model inputs

The model inputs for finding the optimisation results are shown in Table 2. It is worth mentioning that for calculating the emission costs, the South African Carbon Tax was used as no tax or carbon price is yet available in Tanzania. Also, the pollutant costs for the PM$_{2.5}$ and NOx emissions were taken from the estimated external costs reported by IRENA related to the use of fossil fuels for electricity generation and other activities in European countries as no data was found for African countries. It should be noted that seven diesel generators (G1-G7) of different sizes (6.88, 9.76, 14.96, 22.56, 33.76, 44.0, and 143.12 kW) were included for the genset selection, where the smallest power correspond to G1. Finally, it should be mentioned that the price for the repurposed battery (66.95 £/kWh) was assumed to be 50 % of the original Li-ion price according to the second life of batteries scenario presented in the Li-ion batteries for mobility and stationary storage applications report [51].

### 2.4. Economic assessment

The equations presented below, (13) to (17f), were used to carry out an economic assessment based on the life cycle cost (LCC) and the Levelized cost of energy (LCOE) for cost comparison among the electricity generation configurations that appear in section 4. The discounting method was selected, as according to Lai and McCulloch [61] is an appropriate methodology for calculating LCOE when renewable sources are included.

The LCC, also known as Net Present Cost (NPC) for the system within the analysis period $P$ is given by

$$LCC^{system} = LCC^{gen} + LCC^{PV} + LCC^{batt} \tag{13}$$

where $CC^{gen}$, $LCC^{PV}$, and $LCC^{batt}$ are the costs associated with the diesel generators, the PV system, and the battery, respectively. The three terms of the $LCC^{system}$ are defined as follows:

$LCC^{gen}$a): this term includes the costs of the energy generated by the gensets given by

$$LCC^{gen} = LCC^{gen_{load}} + LCC^{gen_{batt}} \tag{14a}$$

$$LCC^{gen_{load}} = \sum_{p \in P} \left( YCF_p^{gen} \cdot df_p \cdot \frac{E_p^{gen_{load}}}{E_p^{gen}} \right) \tag{14b}$$

$$LCC^{gen_{batt}} = \sum_{p \in P} \left( YCF_p^{gen} \cdot df_p \cdot \left( 1 - \frac{E_p^{gen_{load}}}{E_p^{gen}} \right) \right) \tag{14c}$$

$$df = \frac{1}{(1+r)^p} \tag{14d}$$

$$YCF_p^{gen} = \sum_{g \in G} \sum_{bld \in B} \left( C_{g,p=0}^{gen} + C_{bld,g,p}^{fuel} + C_{bld,g,p}^{CO_2e} + C_{bld,g,p}^{NO_x} + C_{bld,g,p}^{PM_{2.5}} + C_{g,p=estglf,estalt}^{r} \right.$$
$$\left. + C_{g,p}^{mnt} \right) \tag{14e}$$

$$estglf = \left( \frac{glf_g}{Hga_g} \right) \cdot iif \quad \frac{P}{\left( \frac{glf_g}{Hga_g} \right)} \le i \le 1 \tag{14f}$$

$$estalt = \left( \frac{20000}{Hga_g} \right) \cdot iif \quad \frac{P}{\left( \frac{20000}{Hga_g} \right)} \le i \le 1 \tag{14 g}$$

where $LCC^{gen_{load}}$ and $LCC^{gen_{batt}}$ are the associated costs of the energy generated by the gensets to supply the load and/or charge the battery. $YCF_p^{gen}$ represents the genset's yearly cash flow, $df$ is the discount factor that considers the real discount rate (10 %). $E_p^{gen_{load}}$ is the electricity delivered by the gensets to the load and $E_p^{gen}$ is the total electricity delivered by the gensets, both in kWh/year. The initial and replacement cost of the gensets are represented by $C_{g,p=0}^{gen}$ and $C_{g,p=estglf,estalt}^{r}$. The estimated engine replacement period ($estglf$) and the estimated alternator replacement period ($estalt$) depend on the lifetime of each engine ($glf_g \in \{3000, 7500\}$) or alternator (20000 h), and their operating hours during the first year of the project ($Hga_g$) as represented in (14f) and (14g). $C_{bld,g,p}^{fuel}$ is the fuel consumption cost, the pollutant emission costs for CO$_2$e, NO$_X$ and PM$_{2.5}$ are represented by $C_{bld,g,p}^{CO_2e}$, $C_{bld,g,p}^{NOx}$, and $C_{bld,g,p}^{PM_{2.5}}$. $C_{g,p}^{mnt}$ is the maintenance cost from (7a).

$LCC^{PV}$b): this term includes the costs of the energy generated by the PV system given by

$$LCC^{PV} = LCC^{PV_{load}} + LCC^{PV_{batt}} \tag{15a}$$

$$LCC^{PV_{load}} = \sum_{p \in P} \left( YCF_p^{PV} \cdot df_p \cdot \frac{E_p^{PV_{load}}}{E_p^{PV}} \right) \tag{15b}$$

$$LCC^{PV_{batt}} = \sum_{p \in P} \left( YCF_p^{PV} \cdot df_p \cdot \left( 1 - \frac{E_p^{PV_{load}}}{E_p^{PV}} \right) \right) \tag{15c}$$

$$YCF_p^{PV} = C_{p=0}^{PV} + C_{p=0}^{inver} + C_{p=20}^{PVrpl} + C_{p=10,20}^{inverpl} \tag{15d}$$

where $LCC^{PV_{load}}$ and $LCC^{PV_{batt}}$ are the associated costs of the energy generated by the PV to supply the load or charge the battery. $YCF_p^{PV}$ represents the PV's yearly cash flow, $E_p^{PV_{load}}$ is the electricity delivered by the PV to the load and $E_p^{PV}$ is the total electricity delivered by the PV, both in kWh/year. $C_{p=0}^{PV}$ and $C_{p=0}^{inver}$ are the initial costs of the PV and the corresponding inverters. Similarly, $C_{p=20}^{PVrpl}$ and $C_{p=10,20}^{inverpl}$ represent their replacement costs.

$LCC^{batt}$c): this term includes the costs of the energy supplied by the batteries given by

$$LCC^{batt} = \sum_{p \in P}^{Y} YCF_p^{batt} \cdot df_p \tag{16a}$$

$$YCF_p^{batt} = C_{p=0}^{batt} + C_{p=battlf}^{battrpl} \tag{16b}$$

where $YCF_p^{batt}$ is the battery system's yearly cash flow, $C_{p=0}^{batt}$ is the battery initial cost and $C_{p=battlf}^{battrpl}$ is its replacement cost. The battery replacement cost depends on the lifetime of a specific battery type,
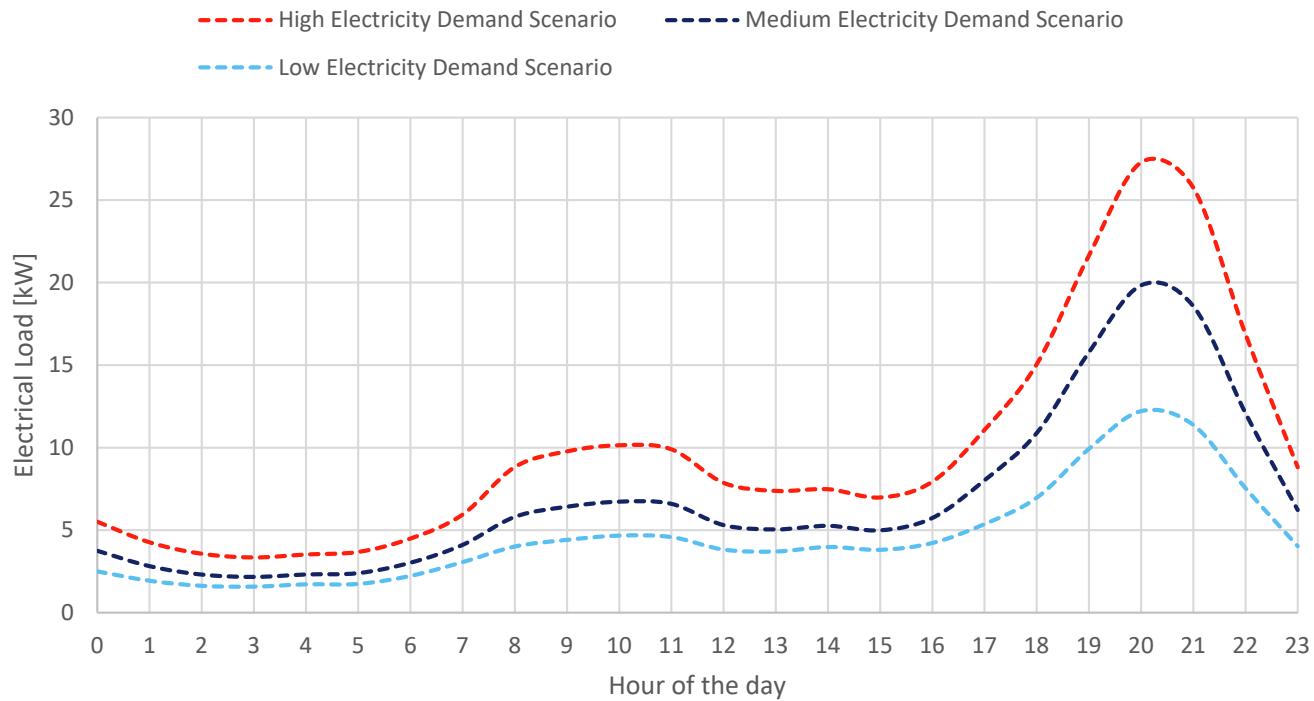
**Fig. 4.** Electricity demand scenarios created for Mpigamiti, Tanzania.

**Table 3**
Relevant data for PV array selection (low, medium, and high installed capacity).

| Electricity Demand Scenario | Average electrical load during daylight (kW) | Peak electrical load (kW) | Min electrical load (kW) | Low PV installed capacity required (kW) | Medium PV installed capacity required (kW) | High PV installed capacity required (kW) |
|---|---|---|---|---|---|---|
| High | 9 | 27 | 3.35 | 5 | 7 | 12 |
| Medium | 6 | 20 | 2.17 | 3 | 5 | 8 |
| Low | 4 | 12 | 1.58 | 2 | 3 | 6 |

which gives different battery replacement periods (*battlf*), in years. For a Lead-acid battery, $battlf \in \{6, 12, 18, 23\}$, for a Li-ion battery, $battlf \in \{10, 20\}$, and for a Repurposed battery, $battlf \in \{5, 10, 15, 20\}$.

Finally, the LCOE of the system is given by

$$LCOE^{system} = \frac{LCC^{system}}{\sum_{p \in P}^{1} \left( E_p^{system} \cdot df_p \right)} \tag{17a}$$

$$E_p^{system} = E_p^{load} + E_p^{batt} \tag{17b}$$

$$E_p^{load} = E_p^{gen_{load}} \left(1 - dr^{gen}\right)^p + E_p^{PV_{load}} \left(1 - dr^{PV}\right)^p \tag{17c}$$

$$E_p^{batt} = \eta \cdot \left( E_p^{gen_{batt}} \left(1 - dr^{gen}\right)^p + E_p^{PV_{batt}} \left(1 - dr^{PV}\right)^p \right) \tag{17d}$$

$$E_p^{gen_{batt}} = E_p^{gen} - E_p^{gen_{load}} \tag{17e}$$

$$E_p^{PV_{batt}} = E_p^{PV} - E_p^{PV_{load}} \tag{17f}$$

where $E_p^{system}$ is the total electricity delivered by the system, $E_p^{load}$ is the electricity delivered by the genset and the PV to the load, and $E_p^{batt}$ is the electricity delivered by the battery to the load, all of them in kWh/year. $\eta$ is the roundtrip efficiency of the battery and $dr$ is the degradation rate [61] considered for each element in the system. Fig. 3 exemplifies the importance of computing $E_p^{system}$ according to (17b), to prevent double counting the electricity delivered from the battery to the load as the battery is not a generating source itself.

## 3. Electricity demand and PV system scenarios

To test the performance of the model, several scenarios were created to present how a different electricity demand profile and the different installed capacity of PV systems, with and without a battery system affect the genset selection for installing a MG in a rural ward (Mpigamiti), located within the Lindi Region of Tanzania.

### 3.1. Electricity demand scenarios

The three load profiles shown in Fig. 4 represent the electricity demand scenarios (high, medium, and low) generated using the Rural African Load Profile Tool developed by the National Renewable Energy Laboratory (NREL) [48]. The load profile tool provides hourly electrical load profiles for different household configurations and commercial facilities (schools, clinics, etc.) as specified by the user inputs. This work considered 350 households with an average household size of 6 people [62] for the 2096 inhabitants in Mpigamiti [63]. The electrical load from the commercial facilities was unchanged across the scenarios but a different percentage of low, medium, and high-income households was considered for comparison purposes. The household configuration and commercial inputs for each scenario and a map showing the Lindi Region (see Fig. S1 [75]) are included in the supplementary material section.

Fig. 4 shows that the profiles from all three scenarios have the similar pattern, i.e. a large peak in the evening (around 20:00) when people starts to switch on electric appliances and a mild peak in the morning. However, the high electricity demand scenario with 70 % high income
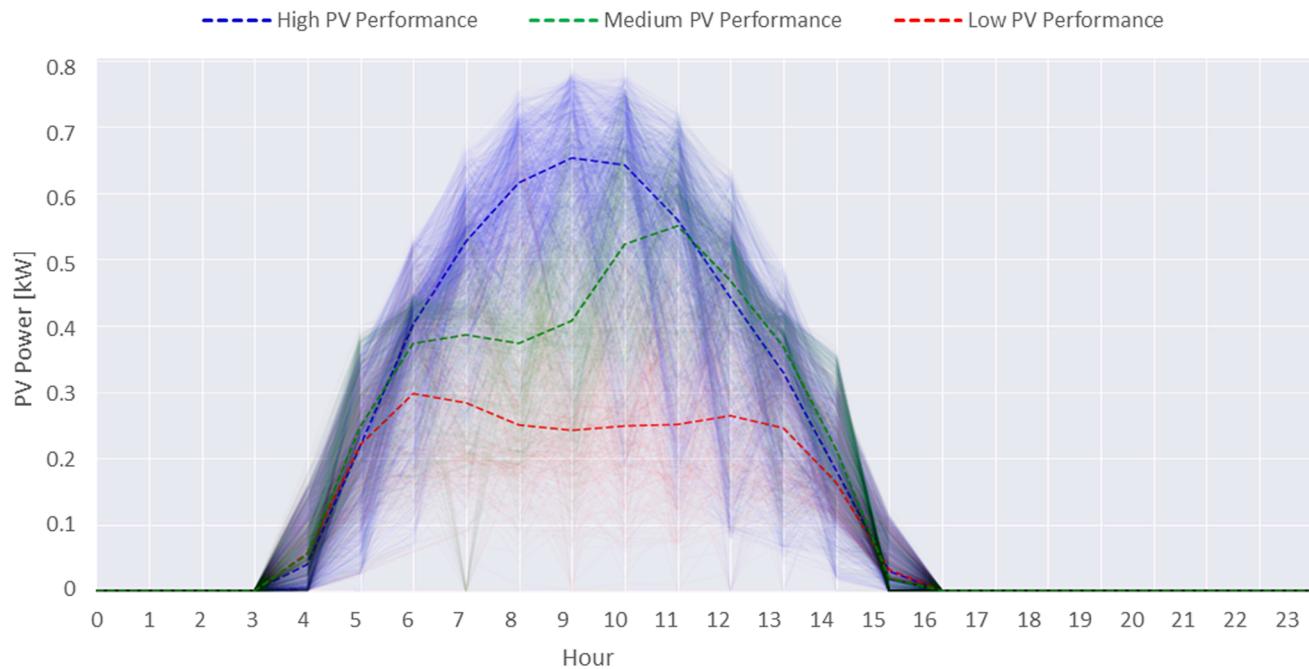
**Fig. 5.** Output power and representative operating day clusters for a 2 kW PV system over five years.

**Table 4**
Examples of optimisation results with fixed PV capacity and performance (regular PV performance and a high PV installed capacity) at High, Medium, and Low load scenarios.

| System configuration | Electricity demand scenario | | |
|---|---|---|---|
| | High (HED) | Medium (MED) | Low (LED) |
| SC1-Genset[**] | G1 + G2 + G3 | | |
| SC2-Genset and PV | G1 + G2 + G3 | | |
| SC3-Genset and Battery (Lead-acid) | G3 | G2 | G1 |
| SC4-Genset and Battery (Li-ion) | G3 | G3 | G1 |
| SC5-Genset and Battery (repurposed) | G4 | G3 | G2 |
| SC6-Genset, PV, and Battery (Lead-acid) | G3 | G2 | G1 |
| SC7-Genset, PV, and Battery (Li-ion) | G3 | G3 | G1 |
| SC8-Genset, PV, and Battery (repurposed) | G1 + G2 | G3 | G2 |

[**] G1: 6.88 kW, G2: 9.76 kW, G3: 14.96 kW. A complete list of the gensets used in the optimisation model is provided in the supplementary material (see Table S4 [76]).

households demonstrated a much higher peak than the low electricity demand scenario because the high-income families have more electric appliances.

### 3.2. PV system scenarios

For the electricity demand scenarios presented above, the average electrical loads during daylight hours, from 7 am to 6 pm, were calculated for selecting the PV system required, able to supply 40 %, 60 %, or 100 % of the average load. The numbers gave three PV scenarios corresponding to a low (40 %), medium (60 %), or high (100 %) PV installed capacity as summarized in Table 3.

### 3.3. PV performance scenarios

For every PV scenario, the hourly output power was calculated using the Photovoltaic Geographical Information System (PVGIS) interactive tool from the European Commission website, with the solar radiation

data from 2016 to 2020 [64]. Once the hourly output power was calculated, the clustering K-Means algorithm from scikit-learn [65] was applied, following the methodology presented in [66], to obtain the representative operating day from each PV system. The representative operating day gives a reasonable estimate of the possible PV system power generation considering the solar radiation fluctuation for the whole year. Fig. 5 shows the clustering for a 2 kW PV system, the blurred lines correspond to the raw daily hourly power output during the five years, and the dashed lines show the three clusters created after grouping the data according to their hourly output values.

The PV cluster diagram is useful to present the possible PV power output scenarios, considering a low, medium and high PV performance as defined by the representative day found with the K-means algorithm. The representative days can be used for scenario analysis to determine how the PV system performance may alter the diesel generator operating conditions. In this work the PV power output was assumed as regular (most likely) for demonstration purposes. The power generation by source and the total power generation diagrams of the hybrid systems (PV, genset, and battery) for each electricity demand profile have been added in the supplementary material to show how the PV power (and the other power sources) relate to the electricity demand profile.

It is worth noting that there are uncertainties linked to the load and the PV generation configuration in the model. Possible uncertainties include:

- assumption of the electrical load from the commercial facilities unchanged across the scenarios which may not be true
- number of households
- fractions of high, medium and low-income households, and the number of commercial facilities.
- assumed installed PV capacity, accuracy of the solar radiation data and the PVGIS tool.

The input uncertainty (since PV generation and Load consumption are considered inputs to the optimisation model) can be characterised with probability functions. The parameters and type of the probability functions can be derived using historical data of the installation location or nearby installations with similar load types and PV characteristics. This approach converts some of the optimisation model constraints into
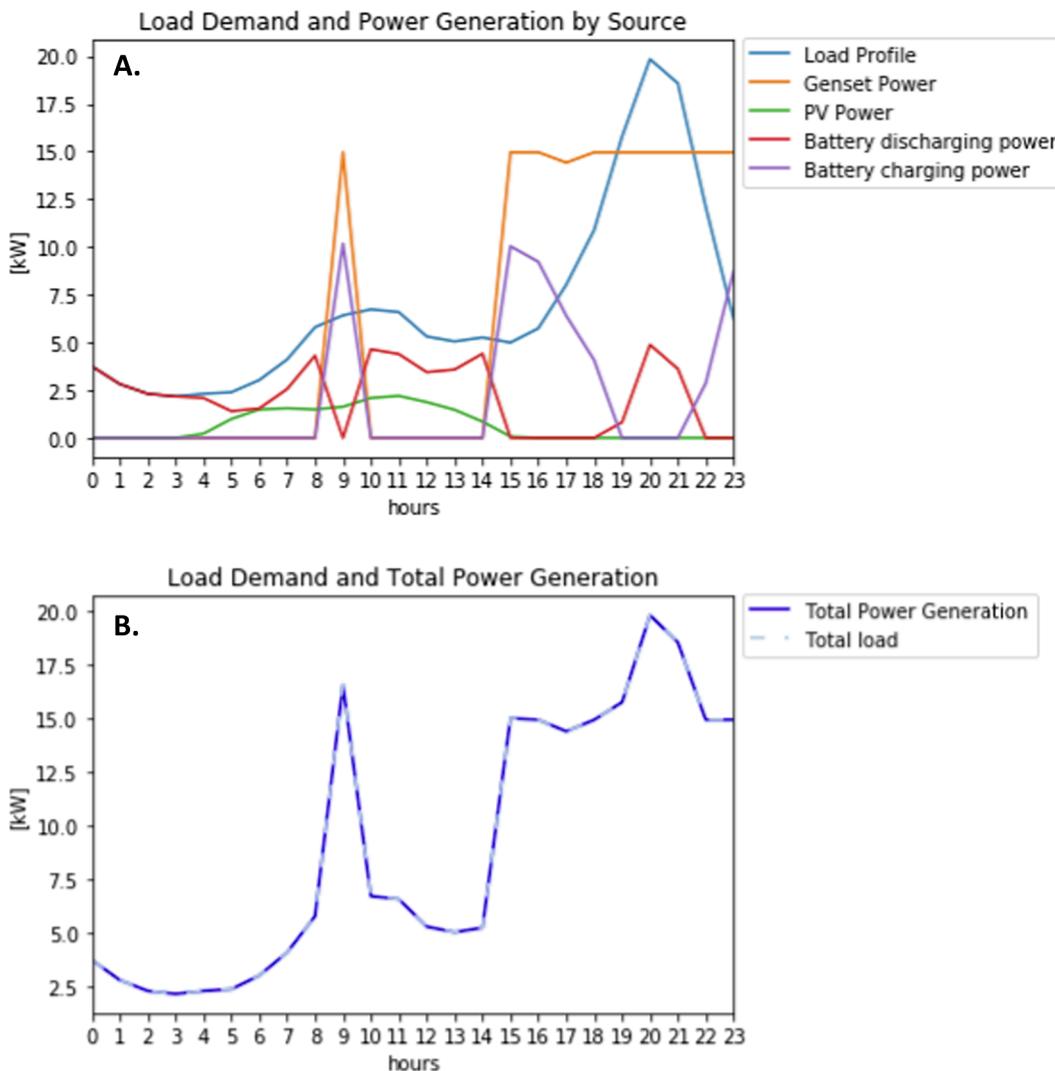
**Fig. 6.** Load demand and power generation by source (A.) and Load demand and total power generation (B.) diagrams for SC8-Genset, PV, and Battery (repurposed) with medium electricity demand profile.

chance constraints. The problem can then be solved as Stochastic MILP or a Robust MILP using many different approaches [67–69]. However, in this work, the expected values of the PV generation and load consumption are used to simplify the solution and focus on the genset selection and characteristics.

## 4. Exemplar application of the tool for optimised hybrid MG configurations at various electricity demands

The proposed tool can be used for the optimal selection of gensets in various system configurations, i.e. which genset or gensets should be selected for a given system configuration (pure genset or hybrids with different PV capacity and performance levels and a variety of battery capacities). For demonstration purposes, an example case was set with fixed PV capacity and performance (regular PV performance and a high PV installed capacity) and a battery installed capacity able to supply the night demand (peak shaving from 6 to 11 pm). The proposed tool was used for optimised Genset selection for eight system configurations (SC) considered for the high, medium, and low electricity demand (HED, MED, and LED) scenarios, as shown in Table 4. Here, all three demand scenarios (HED, MED and LED) were included and logically ordered. There is no randomness for the scenario appearance. The computational effort required to find the optimum solution was between 2370 and 1,087,385 simplex iterations depending on the system configuration

that was optimised. The optimisation problem has 3376 continuous variables and 1064 integer (binary) variables.

Generation profiles from different system configurations would vary depending on the power generation mix and electricity demand. The full analysis of the generation profiles would require 24 figures, which is not the focus of this paper. However, an example of the optimised power generation profile of a hybrid system SC8-Genset, PV, and Battery (repurposed) for a medium electricity demand is shown in Fig. 6. Fig. 6A shows the optimised power contribution of each generating source as well as the power required to charge the batteries. The load demand and total power generation (Fig. 6B) indicates that the optimisation process was successfully carried out as it shows a perfect match between the power generation curve and the total load curve (electricity demand plus battery charging power). This combined power generation allows fuel savings during the periods when the genset is not working. Moreover, the optimised interaction of the power sources enables to keep the diesel generator operating at the recommended conditions by charging the batteries during the low electricity demand periods or during the periods where the PV system contributes to supply the electricity demand.

Other examples of the power generation profiles for SC6, SC7 and SC8 at HED, MED and LED are presented in Figs. S2-S9 of the supplementary materials. These examples show how the power generation profiles vary according to the electricity demand, the PV system and the
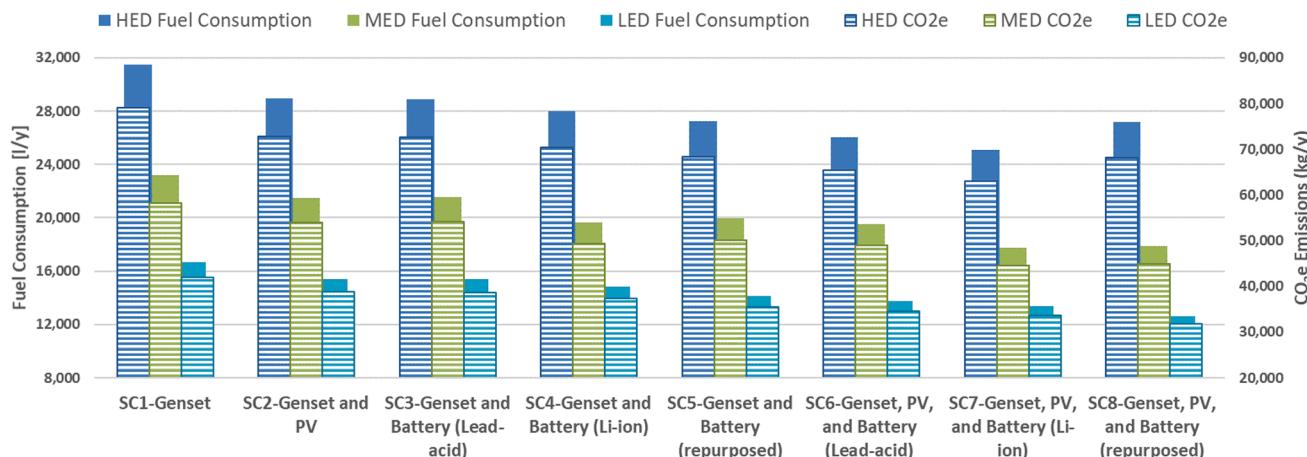
**Fig. 7.** Fuel consumption and CO2e emissions per year for different MG configurations with different electricity demand profiles.
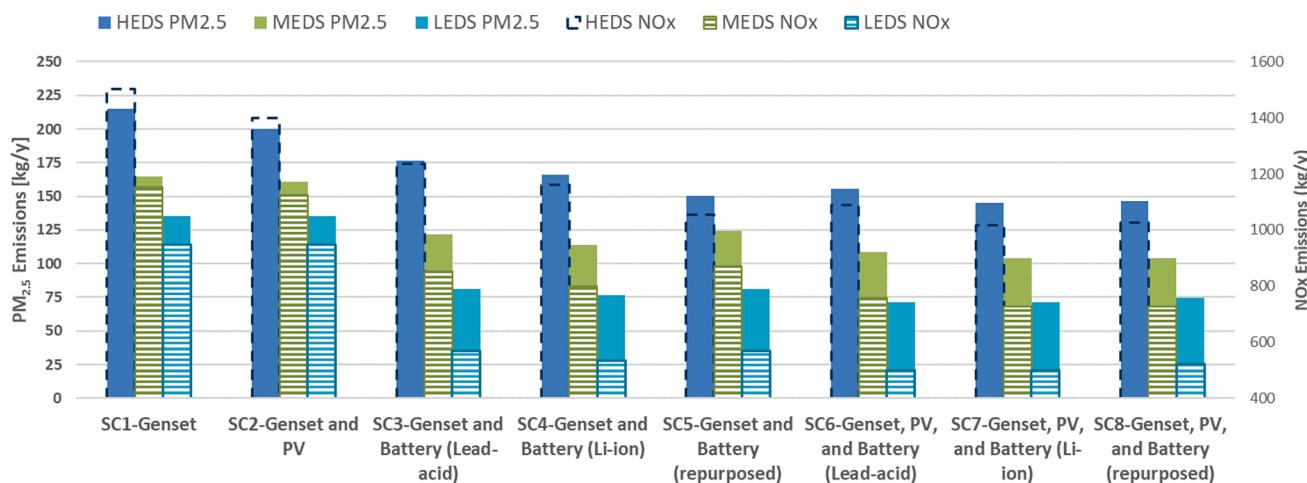


**Fig. 8.** PM$_{2.5}$ and NOx emissions per year for different MG configurations with different load profiles.

installed battery. According to the model constraints, the battery discharges during the night peak to reduce the power generation from diesel generators for reducing fuel consumption and pollutant emissions. The different shape of the power generation profiles is best appreciated in the load demand and total power generation diagrams, where the total power generation curve well matches the total load curve (electricity demand plus battery charging power), indicating that the optimisation process was successfully carried out in all the configurations.

The optimisation results indicate that three diesel generators (G1, G2, and G3) should be installed in the scenarios without a battery to allow the optimum performance of the diesel generators preventing excessive fuel consumption and higher pollutant emissions. On the other hand, if a battery system is included, only one diesel generator is required for the rest of the hybrid configurations, with the exception found in the HED scenario when using a repurposed battery. The generator size selection across the scenarios varied from G1 to G4 as the choice depends on the electricity demand and the battery characteristics, such as its charging-discharging periods. It was noted that despite the low castor oil price (0.44 £/litre), which is 50 % lower than that of diesel (0.88 £/litre), the fuel selected by the model was diesel (COD-0) in the three scenarios for all the system configurations. A very important factor that determines the fuel type selection is the pollutant emission cost. The mathematical expressions supporting the fuel type selection based on the C0$_2$e and PM$_{2.5}$ emissions are given by (5e) and (5j), these equations include the fuel blend emission factor (*bEF$_{bld}$*) in kgCO$_2$e/litre

and the PM$_{2.5}$ emission factor adjustment coefficient (*EFA$_{bld}^{PM_{2.5}}$*) respectively. The *bEF$_{bld}$* considers the CO$_2$e emissions of a fuel blend according to (5f), which uses the values shown in table 2 (2.51233 for diesel and 0.02529 for biofuels). The *EFA$_{bld}^{PM_{2.5}}$* coefficient indicates the PM$_{2.5}$ emissions of a fuel blend relative to the diesel emissions. Through experimental work it was found that the PM$_{2.5}$ emissions increase as the castor oil content increases in the fuel blend. A table with the *EFA$_{bld}^{PM_{2.5}}$* of each fuel type has been included in the supplementary material section for better understanding of the fuel selection done by the model. By looking at the emissions factors mentioned above, it is expected that the model selects the fuel with the least emission factor, i.e., the emission cost plays an important role in the fuel selection process. Therefore, the fuel selection is based on the fuel price, the emission factors and the emission costs. The model would always select the fuel that represents the minimum overall cost after considering those values for each fuel type. Particular cases are included in the sensitivity analysis section to show how the fuel selection can be impacted by varying the fuel price or the emissions cost.

Fig. 7 shows the fuel consumption and CO$_2$e emissions from different system configurations. A linear correlation between fuel consumption and CO$_2$e emissions has been observed which is aligned with the logic and the fact that CO$_2$ emissions are determined by the carbon content in the fuel. So for engines running with a fixed fuel at above medium load factor, which means similar thermal efficiency and is the case in Fig. 7, CO$_2$ emissions are as a function of fuel consumption. Non-CO$_2$
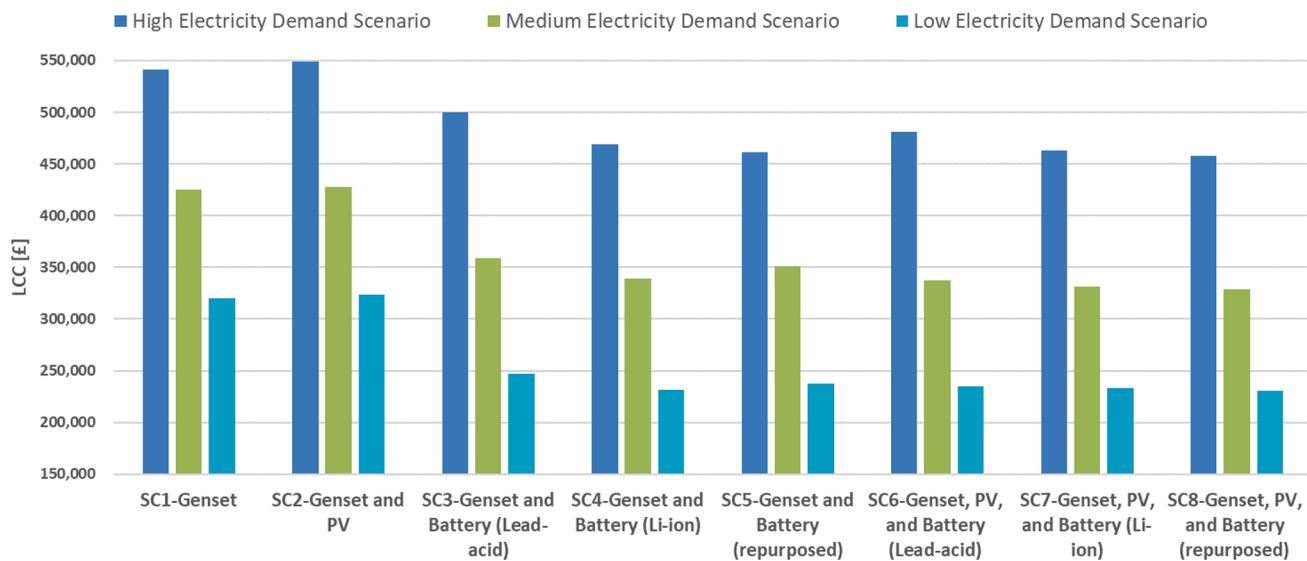
**Fig. 9.** Life Cycle Cost over 25 years for different MG configurations with varying load profiles.
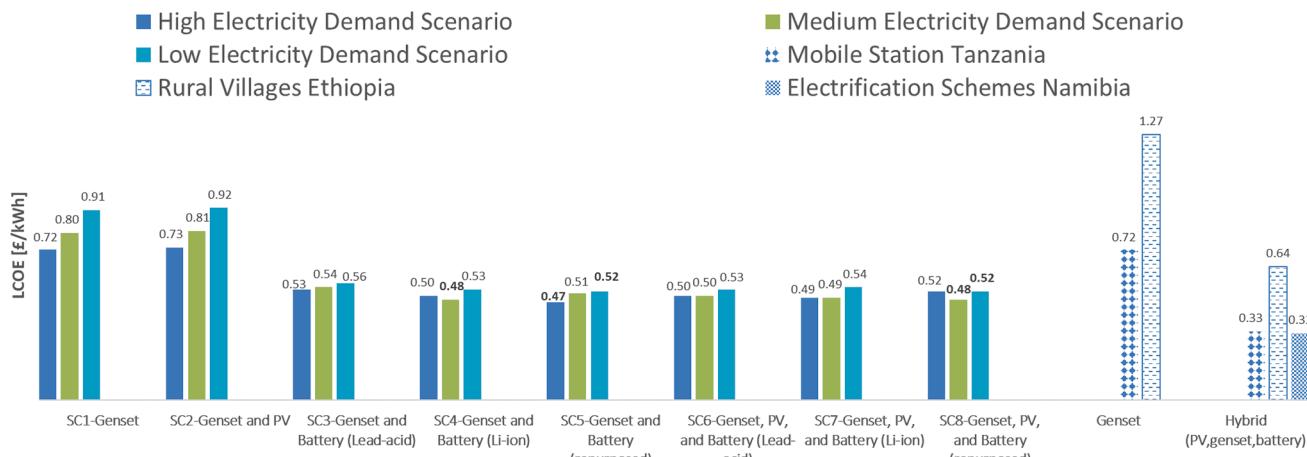


**Fig. 10.** Levelized Cost of Energy over 25 years for different MG configurations with different electricity demand profiles.

emissions, $N_2O$ and $CH_4$, are minimal in the medium to high load combustion of diesel engines so $CO_2$ is the dominant contributor to $CO_2e$ emissions.

Fig. 7 shows that the highest yearly fuel consumption was the SC1-Genset (HED: 31,504.40 l/y, MED: 23,166.60 l/y, and LED: 16,698.80 l/y). As expected, using hybrid configurations (Genset/PV/battery) reduces the fuel consumption for the three scenarios as less energy is required from the diesel generators. It is shown that using SC7-Genset, PV, and Battery (Li-ion) could achieve the lowest fuel consumption, up to 20 % reduction in the HED scenario. In the MED scenario, the lowest fuel consumption could be achieved by SC7 and SC8, up to 23.5 % reduction. In the LED scenario, the SC8-Genset, PV, and Battery (repurposed), has the lowest fuel consumption with up to 24 % reduction. Similar fuel savings were reported in [70], where the total diesel consumption was reduced by about 21 % by replacing a stand-alone diesel generating system with a hybrid PV/Diesel/Battery system. Also, Atmaja et al. [71] reported potential fuel savings between 30 % and 40 % by replacing a 60kVA diesel generator with a smaller one (42kVA) supported by a PV and battery system. The reason that SC7 and SC8 have the lowest fuel consumption is attributed to the combination of PV and lithium-ion battery. In comparison with SC6, where lead acid battery was used, lithium battery (the repurposed battery is the used lithium battery from transport) in SC7 and SC8 has a greater energy

storage capacity than lead acid batteries and is able to provide more electricity and thus reduce fuel consumption. Compared to SC4 and SC5 which only have lithium batteries without PV, electricity from PVs in SC7 and SC8 resulted in more reductions in fuel consumption.

Correspondingly to the fuel consumption, the highest $CO_2e$ emissions (HED: 79,149.40 kg/y, MED: 58,202.00 kg/y, and LED: 41,952.80 kg/y) were also found in the SC1-Genset. Therefore, the emissions could be reduced by 20 %, 23.5 %, and 24 % in the HED, MED and LED scenarios, respectively. These emissions reduction findings are comparable to the carbon dioxide emissions reduction of about 21 % reported by Lau et al. [70] after implementing a hybrid PV/Diesel /Battery system.

The results in Fig. 7 show the importance of combination of renewable electricity generation (PV) and energy storage (batteries) in reducing fuel consumption in the hybrid microgrid systems. The larger the capacity of the energy storage, the lower the fuel consumption and emissions.

Similarly, the highest pollutant emission values for $PM_{2.5}$ (HED:214.71 kg/y, MED: 164.83 kg/y, LED: 135.32 kg/y) and NOx (HED: 1,502.95 kg/y, MED: 1,153.82 kg/y, LED: 947.21 kg/y) were found in the SC1-Genset. Fig. 8 shows the $PM_{2.5}$ and NOx emission values found for the different configurations. The figures indicate that both pollutants can be reduced up to 47 % in the LED scenario with the SC6-Genset, PV, and Battery (Lead-acid) or the SC7-Genset (Li-ion). A
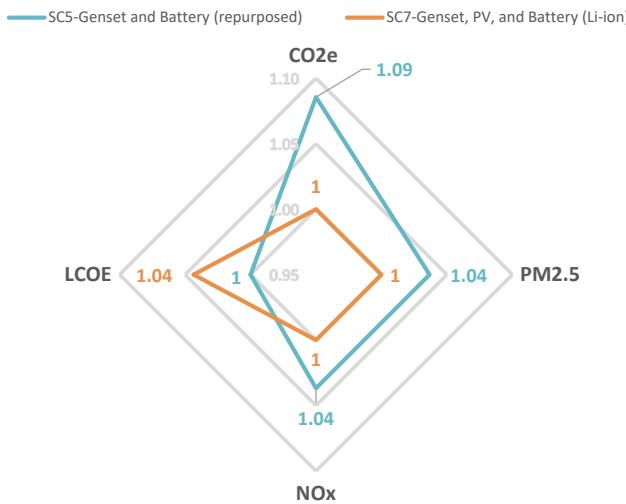
**Fig. 11.** Pollutant emissions and LCOE comparison for selected HED scenario hybrid system configurations. SC7 has the lowest emissions while SC5 has the lowest LCOE.



**Fig. 13.** Pollutant emissions and LCOE comparison for selected LED scenario hybrid system configurations. SC6 and SC7 have the lowest NOx and PM$_{2.5}$ emissions. SC8 has the lowest CO$_2$e emissions. SC5 and SC8 have the lowest LCOE.

**Table 5**
Pollutant emissions and LCOE baseline values (the lowest of each category) considered for the cost-benefit analysis presented in Figs. 11, 12, and 13.

| Scenario | CO$_2$e Emissions Baseline (kg/y) | PM$_{2.5}$ Emissions Baseline (kg/y) | NOx Emissions Baseline (kg/y) | LCOE-25 years Baseline (£/kWh) |
|---|---|---|---|---|
| HED | 62,994.90 | 145.25 | 1,016.73 | 0.47 |
| MED | 44,535.30 | 103.75 | 726.23 | 0.48 |
| LED | 31,794.30 | 71.57 | 500.98 | 0.52 |



**Fig. 12.** Pollutant emissions and LCOE comparison for selected MED scenario hybrid system configurations. SC7 has the lowest emissions while SC4 and SC8 have the lowest LCOE.

37 % reduction is possible in the MED scenario using the SC7-Genset, PV, and Battery (Li-ion) or the SC8-Genset, PV, and Battery (repurposed). In the HED scenario, these pollutant emissions can be reduced by 32 % with the SC7-Genset, PV, and Battery (Li-ion).

It should be noted that the higher reduction in pollutant emissions for PM$_{2.5}$ and NOx compared to the CO$_2$e reduction is attributed to the size of the diesel generators that play an essential role in (5h) and (5j) for the emission calculations. This means that the size of any generator considered within the hybrid systems (G1, G2, G3 or G1 + G2) will give lower PM$_{2.5}$ and NOx emissions than those from the SC1-Genset with a higher installed capacity (G1 + G2 + G3). The size effect is not reflected on the CO$_2$e emissions as they are calculated from the fuel consumption computed in (5d) in terms of the Genset's operating power rather than on the actual generator's size.

## 5. Economic assessment

An economic evaluation among the optimised MG configurations from the previous section was conducted to determine which system can

**Table 6**
LCOE Sensitivity analysis input values with a brief description.

| Modified Parameter | Low Cost | High Cost | |
|---|---|---|---|
| Diesel Price (£/l) * | 0.441 | 1.765 | It was considered a 50 % reduction (low cost) and a two-times increase (high cost) from the current price (0.88 £/l). |
| Carbon Tax (£/kgCO2e) * | 0 | 0.1497 | It was considered a zero-carbon tax (low cost) and a 20 times increase (high cost) in the current South African carbon tax (9.84 US/tCO$_2$e), which equals the highest existing carbon tax in the world (Uruguay:137.30 US/tCO$_2$e) [54]. The baseline cost was 0.0075 £/kgCO$_2$e, as reported in Table 2. |
| PM$_{2.5}$ Emissions (£/gPM2.5) * | 0 | 0.1519 | It was considered a zero PM$_{2.5}$ emission cost (low cost) and the high cost of 199,630 USD/tonne [56]. The baseline cost was 0.0527 £/g, as reported in Table 2. |
| NOx Emissions (£/gNOx) * | 0 | 0.0243 | It was considered a zero NOx emission cost (low cost) and the high cost of 31,941 USD/tonne [56]. The baseline cost was 0.0089 £/g, as reported in Table 2. |

* Prices converted to £ from their original values in USD, considering the average exchange rate history of 1 USD=0.76079 GBP (Dec-May 2022) [60].

present more benefits considering financial and environmental implications. Fig. 9 shows the overall cost comparison for a Life Cycle Cost (LCC) over a 25-year horizon. The numbers indicate that the highest LCC corresponds to the SC2-Genset and PV in all the electricity demand scenarios (HED: £549,457.78, MED: £427,943.46, and LED: £323,644.75). These high costs are attributed to the high fuel

**A.** Sensitivity Analysis for the HED Profile: SC1-Genset

■ Low Cost  ■ High Cost

| | Low Cost | High Cost |
|---|---|---|
| PM2.5, NOx, and Carbon Tax | 0.32 | 1.37 |
| PM2.5 and NOx | 0.32 | 1.24 |
| NOx | 0.56 | 0.99 |
| PM2.5 | 0.51 | 0.97 |
| Carbon Tax | 0.71 | 0.85 |
| Diesel | 0.56 | 0.98 |

0.3  0.37  0.44  0.51  0.58  0.65  0.72  0.79  0.86  0.93  1  1.07  1.14  1.21  1.28  1.35  1.42
**LCOE (£/kWh)**

**B.** Sensitivity Analysis for the HED Profile: SC7-Genset,PV, and Battery (Li-ion)

■ Low Cost  ■ High Cost

| | Low Cost | High Cost |
|---|---|---|
| PM2.5, NOx, and Carbon Tax | 0.27 | 0.86 |
| PM2.5 and NOx | 0.27 | 0.77 |
| NOx | 0.4 | 0.63 |
| PM2.5 | 0.36 | 0.62 |
| Carbon Tax | 0.48 | 0.57 |
| Diesel | 0.38 | 0.64 |

0.24  0.29  0.34  0.39  0.44  0.49  0.54  0.59  0.64  0.69  0.74  0.79  0.84  0.89
**LCOE (£/kWh)**
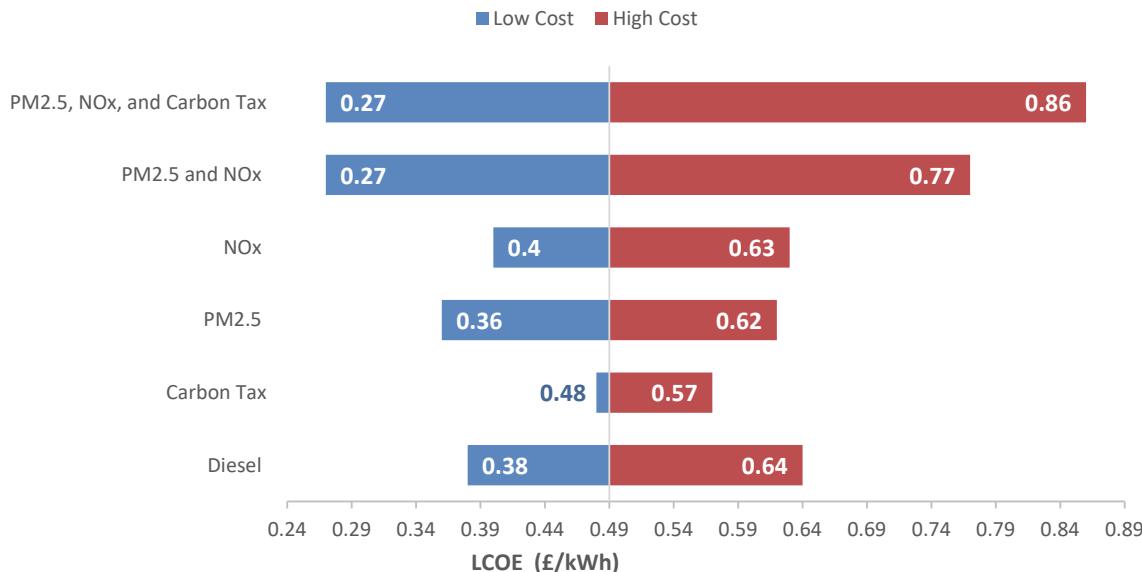
**Fig. 14.** LCOE (£/kWh) sensitivity analysis for two system configurations in the HED scenario: A. SC1-Genset and B. SC7-Genset, PV, and Battery (Li-ion).
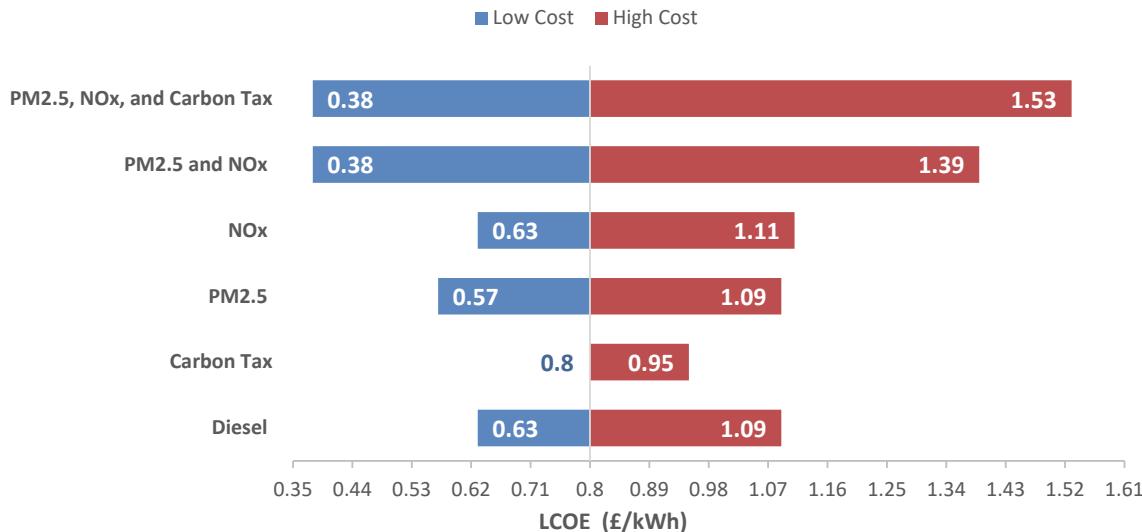
consumption plus the initial investment on PV arrays that do not help to reduce the diesel generators' operating hours during the night peak as PVs are not generating electricity in the night and there are no energy storage systems (batteries). The LCC is comprised of initial purchase costs, maintenance and part replacement costs and fuel costs. The cost of fuel during the assessed period (25 years) is a dominant factor for the LCC so results in Fig. 9 have the similar pattern as Fig. 7.

Overall, it can be seen that adding batteries to the MG systems has a significant impact on LCC values for all electricity demand scenarios. This is because adding batteries reduced the number of generators needed, i.e. three generators were selected in SC1 and SC2 whereas only one generator was selected for the rest of configurations. Therefore, it is recommended that including energy storage systems to microgrids is important for reducing the LCC values. The lowest LCC was found in the SC8-Genset, PV, and Battery (repurposed) for the three scenarios (HED: £ 457,929.81, MED: £328,786.48, and LED: 230,541.23). Those values corresponded to 16.7 %, 23 %, and 28.8 % reductions in LCC,

respectively, compared to the reference configuration (SC2-Genset and PV). A slightly higher LCC for SC7 is due to higher costs of new lithium batteries compared to repurposed lithium batteries in SC8 (£133.9/kWh for new and £66.95/kWh for repurposed). In the high electricity demand scenario, SC5 is also competitive due to that the fuel consumption in Fig. 7 for SC5 and SC8 is similar, which confirms that the fuel consumption is a dominant factor for LCC. Inclusion of PVs in SC6-8 did not vary the LCC significantly, indicating that the additional cost from the installation of PVs would not increase the overall costs.

As presented above, the LCC determined the cheapest configuration over the useful life of different system configurations, but it didńt reflect a fair comparison in terms of per unit of electricity generation for the diverse technologies included. Therefore, a second comparison, over the same 25-year horizon, based on the overall cost and the total electricity produced by each SC was done using the Levelized Cost of Energy. Fig. 10 shows the LCOE of each SC within the three electricity demand scenarios. The best value for the HED scenario (0.47 £/kWh) was found

**A. Sensitivity Analysis for the MED Profile: SC1-Genset**

■ Low Cost  ■ High Cost

| Category | Low Cost | High Cost |
|---|---|---|
| PM2.5, NOx, and Carbon Tax | 0.38 | 1.53 |
| PM2.5 and NOx | 0.38 | 1.39 |
| NOx | 0.63 | 1.11 |
| PM2.5 | 0.57 | 1.09 |
| Carbon Tax | 0.8 | 0.95 |
| Diesel | 0.63 | 1.09 |

X-axis: 0.35 0.44 0.53 0.62 0.71 0.8 0.89 0.98 1.07 1.16 1.25 1.34 1.43 1.52 1.61

**LCOE (£/kWh)**

**B. Sensitivity Analysis for the MED Profile: SC7-Genset, PV, and Battery (Li-ion)**

■ Low Cost  ■ High Cost

| Category | Low Cost | High Cost |
|---|---|---|
| PM2.5, NOx, and Carbon Tax | 0.27 | 0.86 |
| PM2.5 and NOx | 0.27 | 0.77 |
| NOx | 0.4 | 0.64 |
| PM2.5 | 0.36 | 0.62 |
| Carbon Tax | 0.48 | 0.57 |
| Diesel | 0.38 | 0.58 |

X-axis: 0.24 0.29 0.34 0.39 0.44 0.49 0.54 0.59 0.64 0.69 0.74 0.79 0.84 0.89
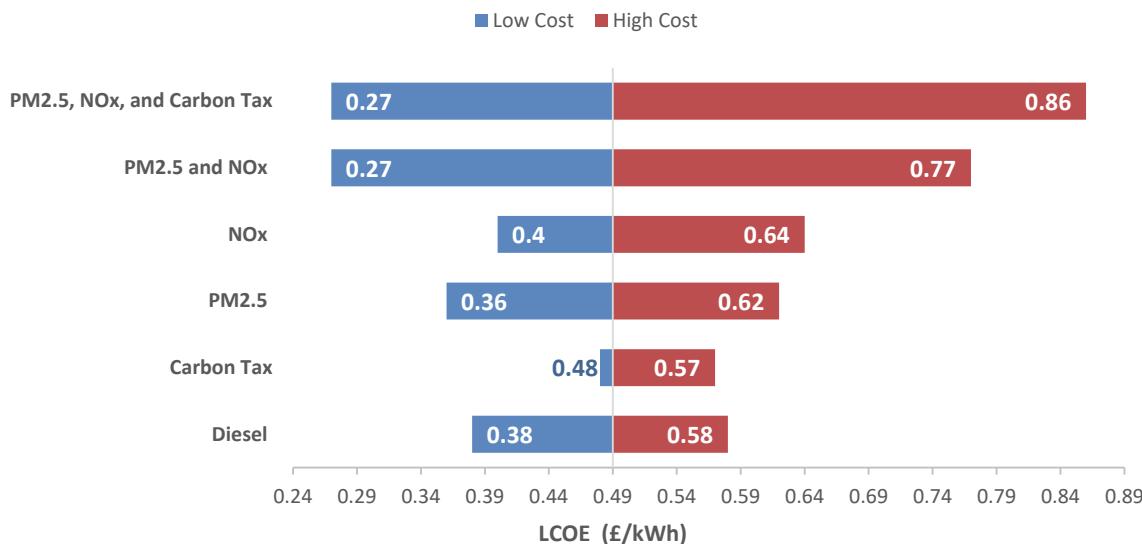
**LCOE (£/kWh)**

**Fig. 15.** LCOE (£/kWh) sensitivity analysis for two system configurations in the MED scenario: A. SC1-Genset and B. SC7-Genset, PV, and Battery (Li-ion).
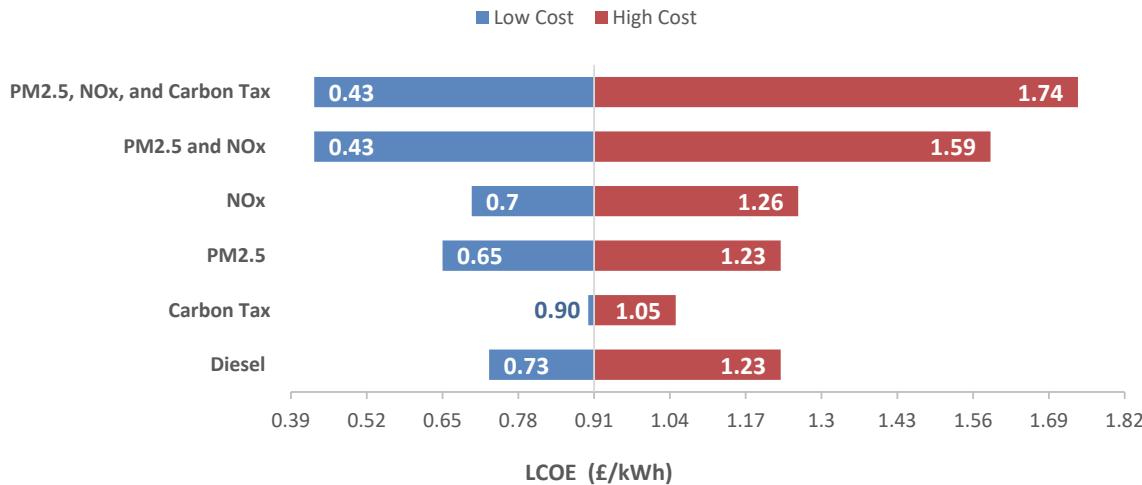
in the SC5-Genset and the Battery (repurposed). The MED scenario showed the best value (0.48 £/kWh) in in two configurations, the SC4 and the SC8. For the LED scenario, the best value (0.52 £/kWh) appeared in the two configurations with the repurposed battery system (SC5 and SC8).

These LCOE results showed a similar trend as that reported for an off-grid mobile base station in Tanzania [72] where a hybrid Genset/PV/battery configuration gives the lowest LCOE of 0.433 USD/kWh (0.33 £/kWh) when compared against a Genset configuration with LCOE of 0.945 USD/kWh (0.72 £/kWh). Similarly, the results from a case study in three rural villages in Ethiopia [73] showed that the LCOE of 1.673 USD/kWh (1.27 £/kWh) from a Genset configuration is less favourable than the 0.84, 0.90, and 1.00 USD/kWh (0.64, 0.68, 0.76 £/kWh) LCOE values reported for the hybrid systems considered in that study. Also, similar LCOE results were found in the techno-economic analysis done by Amupolo et al [74], the values reported by the authors were 0.386 USD/kWh and 0.388 USD/kWh which are about 0.32 £/kWh. Those were the best LCOE values found and correspond to the hybrid systems

comprising solar PV, a diesel generator and a battery system for electrification schemes in Namibia. Despite the similarity found in the LCOE trend from this work and the studies cited above, it cannot be ignored that the LCOE values in this work are slightly different. The difference in the results can be attributed to the pollutant emissions costs considered in this optimisation, which are neglected in the other studies. The difference is also attributed to the lower electricity load demand considered by the other authors, which is only about half of the load profile considered for the LED scenario presented in this work.

Given that more than one configuration appeared to have the lowest LCOE, a cost-benefit assessment was needed to fully understand what hybrid configuration might bring more benefits (financial and environmental). The cost-benefit analysis was done by comparing the lowest pollution system in terms of $CO_2e$, NOx, and $PM_{2.5}$ emissions versus the systems with the lowest LCOE highlighted in Fig. 10. The results are shown in Fig. 11, Fig. 12, and Fig. 13, in a form of normalised values, normalised to the baseline or the lowest value for each category ($CO_2e$, $PM_{2.5}$, NOx, and LCOE respectively). The baseline values for each

**A.** Sensitivity Analysis for the LED Profile: SC1-Genset



**B.** Sensitivity Analysis for the LED Profile: SC8-Genset, PV, and Battery (repurposed)
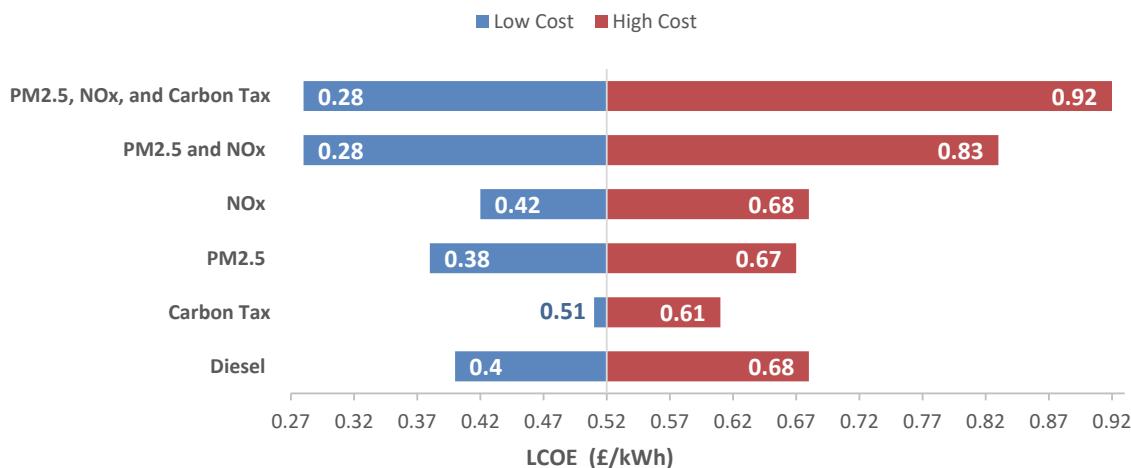


**Fig. 16.** LCOE (£/kWh) sensitivity analysis for two system configurations in the LED scenario: A. SC1-Genset and B. SC8-Genset, PV, and Battery (repurposed).

category are summarised in Table 5.

The results for the HED scenario (see Fig. 11) showed that by selecting SC7, which has the lowest pollutant emissions ($CO_2e$, NOx, and $PM_{2.5}$), the LCOE would be 4 % higher than the LCOE baseline (SC5). If, on the other hand, the SC5 with the lowest LCOE is selected, then the $CO_2e$, $PM_{2.5}$, and NOx emissions would be 9 % and 4 % higher, respectively, when compared to the system with the lowest pollutant emissions (SC7). Therefore, based on the possible increase in pollutant emissions and LCOE values, option SC7 might be a convenient choice for the HED scenario if the environmental benefit is prioritised.

The results for the MED scenario (see Fig. 12) showed that when the environmental benefit is prioritised, SC7 should be selected. The SC7 configuration only represents a 2 % increase in the LCOE value compared to the lowest LCOE found in SC4 and SC8. However, even if the financial benefit is prioritised, SC8 would be an acceptable choice as it only represents a 1 % increase in $CO_2e$ emissions, whereas NOx and $PM_{2.5}$ remained unchanged from the best environmental option (SC7).

Finally, in the LED scenario, the results showed that four configurations should be considered in the cost-benefit analysis (see Fig. 13). The numbers suggest that if the financial benefit is prioritised, then SC5 or SC8 should be selected. At the same time, if the environmental benefit is prioritised (with the focus on $CO_2e$ abatement), then SC8 is still the best option as it generates 6 % and 12 % less CO2e, compared to SC7 and

SC6, respectively. However, it should be noted that the $PM_{2.5}$ and NOx emissions from SC8 are 4 % higher than their respective baseline emissions found in SC6 and SC7.

## 6. Sensitivity analysis

A sensitivity analysis on the LCOE was carried out by the optimisation model using modified diesel prices and pollutant emission costs (carbon tax, $PM_{2.5}$, and NOx). The castor oil price was kept constant as it was inferred from the optimisation results that increasing its price would lead to the same fuel selection (COD-0), as presented in section 4. Table 6 shows the low and high values used in the sensitivity analysis.

The sensitivity analysis was performed for the hybrid configurations with the lowest $CO_2e$ emissions (HED: SC7, MED: SC7, and LED: SC8) and for the corresponding SC1-Genset configuration per electricity demand scenario. The selected configurations for the sensitivity analysis are the most representative systems within each scenario that allow a straightforward LCOE comparison between the conventional and the hybrid MG systems optimised in this work.

Fig. 14 shows the sensitivity analysis results for the HED scenario. In the SC1 analysis (see Fig. 14 A.), it was found that when only one parameter was modified at a time (diesel price, Carbon tax, $PM_{2.5}$ emission cost or NOx emission cost), the scenario with zero-$PM_{2.5}$ cost

produced lower LCOE at 0.51 £/kWh. In contrast, the scenario with high NOx cost gave a higher LCOE value of 0.99 £/kWh. However, when two pollutant emission parameters were set to zero ($PM_{2.5}$ and NOx emission costs), the real lowest LCOE (0.32 £/kWh) was found. This value remained unchanged when the three pollutants' costs were set to zero. When those costs were set to their highest value, the worst LCOE was found (1.37 £/kWh). It should be noted that when the carbon tax was set to zero, almost no variation was observed in the LCOE. In the SC7 analysis (see Fig. 14 B.), a similar trend was found, but the best LCOE was 0.27 £/kWh, and the highest was 0.86 £/kWh. In both SC, diesel was the preferred fuel selected by the model. It was found that only for the high diesel price and for all the cases where the $PM_{2.5}$ emission cost was set to zero, the fuel blend with 50 % castor oil (COD-50) was selected. It was also found that only with the high carbon tax cost, the fuel with 40 % castor oil was selected (COD-40).

Fig. 15 shows the sensitivity analysis results for the MED scenario. In the SC1 analysis (see Fig. 15A.), a favourable LCOE of 0.57 £/kWh appeared with the zero- $PM_{2.5}$ emission cost and a less favourable LCOE of 1.11 £/kWh appeared with the high NOx cost when only one parameter was varied at a time. The best LCOE (0.38 £/kWh) and the worst LCOE (1.53 £/kWh) were found when the three pollutants were set to zero and their highest values, respectively. The results for SC7 (see Fig. 15B.) show that the best LCOE went down to 0.27 £/kWh whereas the highest LCOE was 0.86 £/kWh. Similarly to the HED scenario analysis, it was found that COD-50 was selected for all the cases with zero cost of $PM_{2.5}$ emissions and high diesel price options; and COD-40 was selected when the high carbon tax cost was assessed.

The sensitivity analysis results for the LED scenario are shown in Fig. 16. In the SC1 results (see Fig. 16A.), a favourable LCOE of 0.65 £/kWh appeared with the zero $PM_{2.5}$ emission cost, and a less favourable LCOE (1.26 £/kWh) appeared with the high NOx cost when only one parameter was varied at a time. The best LCOE (0.43 £/kWh) and the worst LCOE (1.74 £/kWh) were found when the three pollutants were set to zero and their highest value, respectively. It should be noted that again, only a small variation was observed in the LCOE when the carbon tax was set to zero. The results for the SC8 (see Fig. 16B.) show that the best LCOE was 0.28 £/kWh, and the worst LCOE was 0.92 £/kWh. Finally, as in the previous scenarios, it was found that COD-50 was selected by the model for all the cases where the $PM_{2.5}$ cost was set to zero and for the option with the high diesel price. Also, as expected, COD-40 was selected with the high carbon tax cost.

## 7. Conclusions

This work presented a cost optimisation model created to improve the performance of diesel generators to be installed within hybrid MGs with different electricity demand scenarios (HED, MED, and LED) in the sub-Saharan African context for eight possible system configurations. The model considered 60 % of diesel generators' prime power as one of the operating limit constraints for avoiding oversized generators and reducing the low load operating conditions, reducing their environmental impact and LCOE. The model included a new set of equations for a better fuel consumption estimation considering the effect of castor oil-diesel blends as no work, to the authors' knowledge, has assessed the effect of these blends in a cost optimisation problem for hybrid MGs design. The model also incorporated $PM_{2.5}$ and NOx emissions for assessing the impact of the emission costs on the fuel blend selection and the LCOE values.

From the cost optimisation results, it was concluded that for the MED and LED scenarios, if no battery was included in the design, more than one Genset was required to avoid oversized diesel generators. The latter was also true for the HED scenario; however, more than one diesel generator would also be needed in the SC8-Genset, PV, and Battery (repurposed).

The economic analysis revealed that the configurations with the best LCOE (HED: SC5, MED: SC8, and LED: SC5 and SC8) do not always

match the configurations with the major environmental benefit from $CO_2e$ reduction (HED: SC7(20 %), MED: SC7 (23.5 %), and LED: SC8 (24 %)). The sensitivity analysis determined that $PM_{2.5}$ and $NO_X$ emission costs have a major impact on the LCOE and that the fuel selection is highly impacted by the $PM_{2.5}$ costs. Therefore, the findings of this work highlighted the importance of considering the effect of pollutant emission costs in optimisation models, especially if biofuel blends are to be used in hybrid systems.

Including these pollutant emission costs, and more fuel choices allows for a better assessment of diesel generators' performance, which could benefit the design of MGs. Furthermore, in the coming years, solar and solar-hybrid micro and MG systems will play an essential role in expanding electricity access in rural areas, and diesel generators are the basic components of such systems. Therefore, reducing diesel generators' operating costs and improving their performance will contribute to better hybrid systems development.

## CRediT authorship contribution statement

**N. Rangel:** Conceptualization, Methodology, Software, Validation, Investigation, Data curation, Writing – original draft, Visualization. **H. Li:** Writing – review & editing, Supervision. **P. Aristidou:** Writing – review & editing, Supervision.

## Declaration of Competing Interest

The authors declare that they have no known competing financial interests or personal relationships that could have appeared to influence the work reported in this paper.

## Data availability

Data will be made available on request.

## Acknowledgments

## Appendix A. Supplementary data

Supplementary data to this article can be found online at https://doi.org/10.1016/j.apenergy.2023.120748.

## References

[1] Ensure Access to Affordable, Reliable, Sustainable and Modern Energy for All. United Nations.

[2] Africa Energy Outlook 2019. International Energy Agency; 2019.

[3] Knuckles J. State of the Mini Grid Market Globally Mini Grids for Half a Billion People. World Bank Group; 2019.

[4] Mini Grids for Half a Billion People : Market Outlook and Handbook for Decision Makers . ESMAP Technical Report;014/19. Washington, DC: World Bank; 2019.

[5] Dimitriou A, Kotsampopoulos P, Hatziargyriou N. Best practices of rural electrification in developing countries: Technologies and case studies. 2014.

[6] Szabo S, Bódis K, Huld T, Moner-Girona M. Energy solutions in rural Africa: mapping electrification costs of distributed solar and diesel generation versus grid extension. Environ Res Lett 2011;6:034002.

[7] Zhao B, Zhang X, Li P, Wang K, Xue M, Wang C. Optimal sizing, operating strategy and operational experience of a stand-alone microgrid on Dongfushan Island. Appl Energy 2014;113:1656–66.

[8] Yamegueu D, Azoumah Y, Py X, Zongo N. Experimental study of electricity generation by Solar PV/diesel hybrid systems without battery storage for off-grid areas. Renew Energy 2011;36:1780–7.

[9] Sinn M. Cost recovery of isolated microgrids in subSaharan Africa: causalities and prerequisites. Chalmers University of Technology; 2014. Unpublished masters dissertation Göteborg:.

[10] Fu Q, Montoya LF, Solanki A, Nasiri A, Bhavaraju V, Abdallah T, et al. Microgrid generation capacity design with renewables and energy storage addressing power quality and surety. IEEE Trans Smart Grid 2012.

[11] Díaz P, Arias C, Peña R, Sandoval D. Far from the grid: A rural electrification field study. Renew Energy 2010.

[12] Kusakana K, Vermaak H. Hybrid Diesel Generator-battery systems for offgrid rural applications. 2013 IEEE International Conference on Industrial Technology (ICIT). IEEE; 2013.

[13] Soto D. Modeling and measurement of specific fuel consumption in diesel microgrids in Papua. Indonesia Energy for Sustainable Development 2018;45: 180–5.

[14] Schnitzer DA. Microgrids and High-Quality Central Grid Alternatives: Challenges and Imperatives Elucidated by Case Studies and Simulation. Carnegie Mellon University; 2014.

[15] Díaz P, Peña R, Muñoz J, Arias C, Sandoval D. Field analysis of solar PV-based collective systems for rural electrification. Energy 2011.

[16] Booth S, Li X, Baring-Gould I, Kollanyi D, Bharadwaj A, Weston P. Productive use of energy in african micro-grids: Technical and business considerations. 2018.

[17] Kimera R, Okou R, Sebitosi AB, Awodele KO. Considerations for a sustainable hybrid mini-grid system: A case for Wanale village, Uganda. Journal of Energy in Southern Africa 2014.

[18] Mamaghani AH, Escandon SAA, Najafi B, Shirazi A, Rinaldi F. Techno-economic feasibility of photovoltaic, wind, diesel and hybrid electrification systems for off-grid rural electrification in Colombia. Renew Energy 2016.

[19] Mellit A, Kalogirou SA, Hontoria L, Shaari S. Artificial intelligence techniques for sizing photovoltaic systems: A review. Renew Sustain Energy Rev 2009.

[20] Bernal-Agustín JL, Dufo-Lopez R. Simulation and optimization of stand-alone hybrid renewable energy systems. Renew Sustain Energy Rev 2009.

[21] Connolly D, Lund H, Mathiesen BV, Leahy M. A review of computer tools for analysing the integration of renewable energy into various energy systems. Appl Energy 2010.

[22] Sinha S, Chandel S. Review of software tools for hybrid renewable energy systems. Renew Sustain Energy Rev 2014.

[23] Suman GK, Guerrero JM, Roy OP. Optimisation of solar/wind/bio-generator/ diesel/battery based microgrids for rural areas: A PSO-GWO approach. Sustain Cities Soc 2021.

[24] Alramlawi M, Timothy AF, Gabash A, Mohagheghi E, Li P. Optimal operation of pv-diesel microgrid with multiple diesel generators under grid blackouts. 2018 IEEE International Conference on Environment and Electrical Engineering and 2018 IEEE Industrial and Commercial Power Systems Europe (EEEIC/I&CPS Europe): IEEE; 2018.

[25] Pelland S, Turcotte D, Colgate G, Swingler A. Nemiah valley photovoltaic-diesel mini-grid: System performance and fuel saving based on one year of monitored data. IEEE Trans Sustainable Energy 2011;3:167–75.

[26] Kusakana K. Optimal operation of parallel-connected diesel generators for remote electrification through energy management approach. In: 2017 IEEE PES. PowerAfrica: IEEE; 2017. p. 380–4.

[27] Knudsen J, Bendtsen J, Andersen P, Madsen K, Sterregaard C, Rossiter A. Fuel optimization in multiple diesel driven generator power plants. In: 2017 IEEE Conference on Control Technology and Applications. (CCTA): IEEE; 2017. p. 493–8.

[28] Reiniger K, Schott T, Zeidler A. Optimization of hybrid stand-alone systems. European Wind Energy Association Conference and Exhibition 1986.

[29] Skarstein Ø, Uhlen K. Design considerations with respect to long-term diesel saving in wind/diesel plants. Wind Eng 1989:72–87.

[30] Maleki A, Askarzadeh A. Optimal sizing of a PV/wind/diesel system with battery storage for electrification to an off-grid remote region: A case study of Rafsanjan. Iran Sustainable Energy Technologies and Assessments 2014;7:147–53.

[31] Azoumah Y, Yamegueu D, Ginies P, Coulibaly Y, Girard P. Sustainable electricity generation for rural and peri-urban populations of sub-Saharan Africa: the "flexy-energy" concept. Energy Policy 2011;39:131–41.

[32] Rohani G, Nour M. Techno-economical analysis of stand-alone hybrid renewable power system for Ras Musherib in United Arab Emirates. Energy 2014;64:828–41.

[33] Lambert T, Gilman P, Lilienthal P. Micropower system modeling with HOMER. Integration of alternative sources of energy 2006;1:379–85.

[34] Generator Fuel Curve Intercept Coefficient. HOMER Pro 3.14 ed: HOMER Energy.

[35] Ashok S. Optimised model for community-based hybrid energy system. Renew Energy 2007.

[36] Agarwal N, Kumar A. Optimization of grid independent hybrid PV–diesel–battery system for power generation in remote villages of Uttar Pradesh. India Energy for Sustainable Development 2013.

[37] Gan LK, Shek JK, Mueller MA. Hybrid wind–photovoltaic–diesel–battery system sizing tool development using empirical approach, life-cycle cost and performance analysis: A case study in Scotland. Energ Conver Manage 2015;106:479–94.

[38] Mazzola S, Astolfi M, Macchi E. The potential role of solid biomass for rural electrification: A techno economic analysis for a hybrid microgrid in India. Appl Energy 2016;169:370–83.

[39] Kumar A, Sharma S, Verma A. Optimal sizing and multi-energy management strategy for PV-biofuel-based off-grid systems. IET Smart Grid 2019;3:83–97.

[40] Ghenai C, Janajreh I. Design of solar-biomass hybrid microgrid system in Sharjah. Energy Procedia 2016;103:357–62.

[41] Wang C, Liu Y, Li X, Guo L, Qiao L, Lu H. Energy management system for stand-alone diesel-wind-biomass microgrid with energy storage system. Energy 2016;97: 90–104.

[42] Bilal BO, Sambou V, Kébé C, Ndiaye P, Ndongo M. Methodology to Size an Optimal Stand-Alone PV/wind/diesel/battery System Minimizing the Levelized cost of Energy and the CO2 Emissions. Energy Procedia 2012.

[43] The Gurobi Python Modeling and Development Environment. Gurobi Optimization, LLC.

[44] Zhongming Z, Linong L, Wangqiang Z, Wei L. Handbook on Battery Energy Storage System. 2018.

[45] Class A2 Gas Oil Specifications. Crown Oil Ltd.

[46] British Standards Institution: BS2869:2017+A1:2022-Fuel oils for agricultural, domestic and industrial engines and boilers. London: BSI; 2022.

[47] 1.A.4 Non road mobile machinery 2019. European Environment Agency.

[48] Li X, Salasovich J, Reber T. Microgrid Load and LCOE Modelling Results. National Renewable Energy. 2018.

[49] El-Hefnawi SH. Photovoltaic diesel-generator hybrid power system sizing. Renew Energy 1998;13:33–40.

[50] Coleman C. Hybrid power system operational test results: wind/PV/diesel system documentation. Conference Proceedings, Eleventh International Telecommunications Energy Conference: IEEE 1989.

[51] Lebedeva N. Li-ion batteries for mobility and stationary storage applications. Publications Office of the European Union; 2018.

[52] Tanzania Diesel prices.

[53] Wamucii S. Tanzania Castor Oil Prices.

[54] Group TWB. Carbon Pricing Dashboard.

[55] Government conversion factors for company reporting of greenhouse gas emissions. 2021.

[56] The true cost of fossil fuels: Externality cost assessment methodology IRENA; 2016.

[57] Economies E. Electrifying Economies : Detailed Cost Models and Benchmarks.

[58] Reber TJ, Booth SS, Cutler DS, Li X, Salasovich JA. Tariff Considerations for Micro-Grids in Sub-Saharan Africa. National Renewable Energy Lab (NREL), Golden, CO (United States) 2018.

[59] SEforALL B. State of the global Mini-Grid Market Report 2020. Sustainable Energy For All. 2020.

[60] US Dollar (USD) to British Pound (GBP) exchange rate history. Exchange Rates.org. uk.

[61] Lai CS, McCulloch MD. Levelized cost of energy for PV and grid scale energy storage systems. arXiv preprint arXiv:160906000. 2016.

[62] Average household size. Global Data Lab.

[63] Brinkhoff T. Liwale District in Coastal Tanzania.

[64] Commission E. Photovoltaic Geographical Informatin System.

[65] Pedregosa F, Varoquaux G, Gramfort A, Michel V, Thirion B, Grisel O, et al. Scikit-learn: Machine learning in Python. the Journal of machine Learning research 2011; 12:2825–30.

[66] Viola LG. Clustering electricity usage profiles with K-means. 2018 Towards Data Science medium publication. 2018.

[67] Spall JC. Stochastic optimization. Handbook of computational statistics: Springer; 2012. p. 173–201.

[68] Sen S. Algorithms for stochastic mixed-integer programming models. Handbooks Oper Res Management Sci 2005;12:515–58.

[69] Janak SL, Floudas CA. Robust Optimization: Mixed-Integer Linear Programs. 2009.

[70] Lau KY, Yusof M, Arshad S, Anwari M, Yatim A. Performance analysis of hybrid photovoltaic/diesel energy system under Malaysian conditions. Energy 2010;35: 3245–55.

[71] Atmaja TD, Kristi AA, Risdiyanto A, Susanto B, Andriani D, Fujita M, et al. Fuel saving on diesel genset using PV/battery spike cutting in remote area microgrid. MATEC Web of Conferences: EDP Sciences 2018:01045.

[72] Kitindi EJ. Techno-economic and environmental analysis for off-grid mobile base stations electrification with hybrid power system in Tanzania. 2021.

[73] Abraha AH, Kahsay MB, Kimambo CZ. Hybrid solar-wind-diesel systems for rural application in North Ethiopia: case study for three rural villages using HOMER simulation. Momona Ethiopian Journal of Science 2013;5:62–80.

[74] Amupolo A, Nambundunga S, Chowdhury DS, Grün G. Techno-Economic Feasibility of Off-Grid Renewable Energy Electrification Schemes: A Case Study of an Informal Settlement in Namibia. Energies 2022;15:4235.

[75] Group WB. Energy Data.Info Mini-grids Locations in Tanzania.

[76] Power Generators. Generators Online Limited.